Use of Response Surface Metamodels in Damage Identification of Dynamic Structures

1943 - 2003

Los Alamos
NATIONAL LABORATORY

Ideas That Change the World

Use of Response Surface Metamodels in Damage Identification of Dynamic Structures

Amanda L. Cundy

1 9 4 3 - 2 0 0 3

Los Alamos
NATIONAL LABORATORY

Ideas That Change the World

Use of Response Surface Metamodels in
Damage Identification of Dynamic Structures

by

Amanda L. Cundy

Daniel J. Inman, Co-Chair, VPI & SU Mechanical Engineering Dept.
Mahendra P. Singh, Co-Chair, VPI & SU Engineering Sciences and Mechanics Dept.
Romesh C. Batra, VPI & SU Engineering Sciences and Mechanics Dept.
François M. Hemez, Los Alamos National Laboratory, ESA-WR

January 7, 2003

Blacksburg, Virginia

Use of Response Surface Metamodels in
Damage Identification of Dynamic Structures

Amanda L. Cundy

Virginia Polytechnic Institute and State University, 2002

Advisor: Daniel J. Inman

ABSTRACT

The need for low order models capable of performing damage identification has become apparent in many structural dynamics applications where structural health monitoring and damage prognosis programs are implemented. These programs require that damage identification routines have low computational requirements and be reliable with some quantifiable degree of accuracy. Response surface metamodels (RSMs) are proposed to fill this need. Popular in the fields of chemical and industrial engineering, RSMs have only recently been applied in the field of structural dynamics and to date there have been no studies which fully demonstrate the potential of these methods. In this thesis, several RSMs are developed in order to demonstrate the potential of the methodology. They are shown to be robust to noise (experimental variability) and have success in solving the damage identification problem, both locating and quantifying damage with some degree of accuracy, for both linear and nonlinear systems. A very important characteristic of the RSMs developed in this thesis is that they require very little information about the system in order to generate relationships between damage indicators and measureable system responses for both linear and nonlinear structures. As such, the potential of these methods for damage identification has been demonstrated and it is recommended that these methods be developed further.

Acknowledgments

Contents

LIST OF FIGURES

LIST OF TABLES

Chapter 1

INTRODUCTION TO RESPONSE SURFACE METAMODELS OF DYNAMIC STRUCTURAL SYSTEMS

This research addresses the problem of damage identification in dynamic structural systems through the use of response surface metamodels, with careful attention paid to quantification of error. Damage identification is a problem of interest in many engineering industries and is the most fundamental part of structural health monitoring and damage prognosis problems. Damage identification is the problem of locating and quantifying damage in structures. This task may be accomplished through any of various methods; for example, visual inspection, non-destructive evaluation methods, or analysis of time history and frequency response data. Structural health monitoring (SHM) is the process of continuously monitoring a structure for damages that may occur in real-time. An example of this may be sensors in place on a bridge that send data to a remote processing station, where an operator may look for damage on a real-time basis [1]. Damage prognosis takes SHM one step further and answers the question, "Based on the current state of damage, how much remaining life or performance does the structure have?" [2]. This thesis will focus on the application of response surface methods to the fundamental damage identification problem. It will become evident that these methods may then be integrated into SHM and damage prognosis.

The concept of a "metamodel" is introduced as a fast running surrogate model. Usually it is a model that will run in minutes on a single processor desktop PC compared to the hours or days that it may take to run a more detailed simulation on a multi-processor machine. It could be a

traditional reduced order model (as obtained from Guyan Reduction or Craig-Bampton methods), a neural network, or a statistically derived model. Because the aim of this research is to focus on a method that is viable for both linear and nonlinear structures, reduced order modeling methods that rely on modal methods will not be addressed. Neural networks for use in nonlinear structural dynamics problems are being addressed by others and are well documented in the literature, for example [2]. They also have the disadvantage of requiring large amounts of training data. The focus of this thesis will be directed toward statistically derived metamodels, or *response surface metamodels* for use in damage identification applications. Figure 1.1 conceptually demonstrates the area of structural dynamics problems in which it is hoped that response surface methods may be of use. Response surface methods may be employed with low effort and have the potential to be applied to both linear and nonlinear problems.
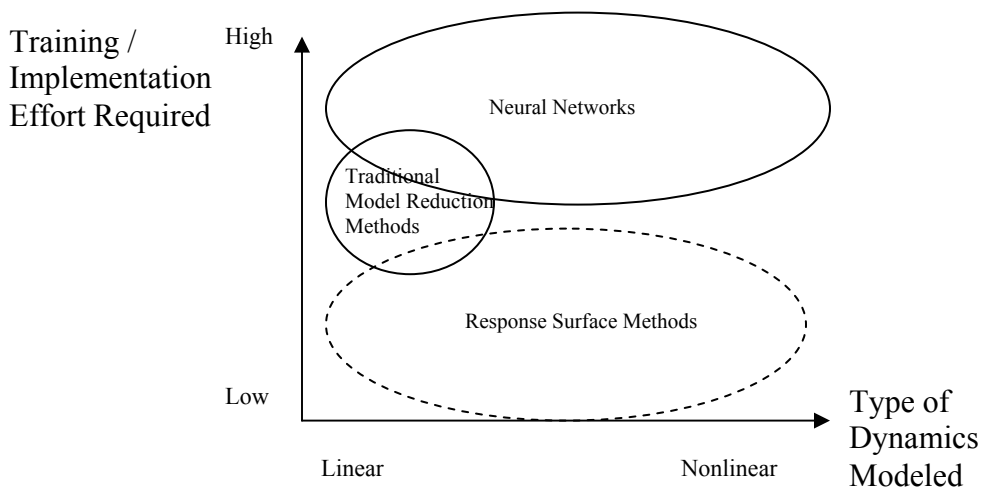
Figure 1.1 Conceptual plot of the types metamodels and problems for which they are suited.

The concept of a *design space* is introduced as the set of all possible experiments or simulations that interest the analyst. This set consists of all controllable variables set at all possible levels and associated dependent features of interest. This space may be n-dimensional in size. Because the total design space is often prohibitively large, methods have been developed in the literature to efficiently explore it.

2

In the case of response surface metamodels, design of experiments methods (often called response surface methods) are employed. Already popular in the chemical and industrial engineering communities, design of experiments is a statistical method used to "intelligently" determine which simulation or physical experiments should be run when resources are scarce [3]. Design of experiments relies on analysis of variance, or ANOVA, to choose a few points out of the full factorial set that efficiently provide information about the full response space. Metamodels may then be fit to these intelligently chosen data points using standard multiple regression methods resulting in a polynomial model that relates input parameters to output features. While these models are empirical in nature, they rely on the expertise of the experimenter for assignment of model input parameters and choice of appropriate output feature(s).

The advantages of using the response surface metamodel formulation are many. Table 1.1 summarizes the abilities of each of the metamodeling methods and it can be seen that response surface methods have many desirable qualities. It is important to understand with response surface metamodels, a numerical model is fitted over a domain, or a range of input parameters. Because of the model form, minimal effort is required to train response surface metamodels and they have relative flexibility in the range of problems they are able to model.

Table 1.1 Advantages and disadvantages of various metamodeling techniques.

	Response Surface Methods	Neural Networks	Traditional Model Reduction Methods
Models linear dynamics?	Yes	Yes	Yes
Models non-linear dynamics?	Yes	Yes	No
Models stochastic phenomenon?	Yes	Yes	No
Data requirement for a given output?	Low	High	Mid
Ability to do damage identification?	Yes - Solving inverse problem required	Yes	Yes - Solving inverse problem required

It is the empirical nature of response surface models that makes them well suited to nonlinear dynamics simulation and experiment, because higher order models may be used to relate input variables to response features. In addition to features derived from the frequency domain (which may be difficult to derive in nonlinear settings), response features may be derived from measured or simulated responses in the time domain. In fact, the number and types of response features used are limited only by the ingenuity of the experimenter.

Another advantage of response surface methods is their ease of implementation in damage identification settings. Relatively few data sets are required to build a model relating inputs and outputs. Because of the large scale of many damage identification projects, engineers rely heavily on simulation because it is often not feasible to conduct many experiments to explore all damage scenarios. (Imagine an aerospace firm fabricating and then destroying 500 airplanes to test all possible damage scenarios!) Additionally, with the advent of programs such as the Department of Energy's ASCI (the Accelerated Strategic Computing Initiative) at National Laboratories across the country, simulations have become increasingly complex, which means they often take tremendous amounts of computing time to run. One example is a simulation of the response of a mechanical joint subject to transient excitation which took 504 processors three hours to run three milliseconds of simulation time on Los Alamos National Laboratory's parallel super computer, Blue Mountain [4]. In many commercial settings, computing power is simply not available to conduct such complex simulations. While having unlimited experiments and/or simulations would be the ideal to explore a dynamic phenomenon, it is easy to see that this may never be the case due to budget and time limitations. Using a small number of data sets (this is equivalent to experiments or simulations), analysts and experimenters may be able to efficiently explore the response space to better determine areas of interest and quantify the variability of predictions.

Use of low order models will have an increasingly important part to play in applications such as structural health monitoring and damage prognosis. These applications may involve putting many sensors on a structure and processing the data onboard, presumably with some kind of minimal hardware. Because of the low training requirements and simple model form of response surface metamodels, they could be used in onboard processing applications, requiring a

minimum of computational power. Damage in the structure might be identified by a response surface model and sent to a remote location where an engineer is monitoring structure status.

In addition to issues of efficiently using small amounts of data, the polynomial nature of metamodeling can make it particularly well suited to the damage identification problem, which is an inverse problem. If several response features are modeled, then these models may be used with an optimization formulation and system inputs may be determined in this inverse fashion. While input formulations may still be non-unique, rating schemes exist which rank the combination of inputs that are most likely to have caused the output features measured. This thesis will explore the use of metamodels in damage identification using these methods.

In order to demonstrate that response surface metamodels may be used in structural damage identification problems two dynamic systems have been examined. Simple problems have been chosen so that an emphasis on the process of metamodel formulation and damage identification may be achieved. Special attention has been given to characterization of error. It will be demonstrated that metamodels show potential for use as reduced order models for damage identification of both linear and nonlinear structural dynamics systems. It will also be shown that response surface metamodels are robust to experimental variability.

The rest of this thesis will be organized as follows. Chapter 2 will address some basic background pertinent to the research of this thesis. Chapter 3 presents a linear five degree-of-freedom (5DOF) spring-mass simulation that was modeled using response surface methods. The resulting metamodel was used to detect and locate damaged springs. The method proved to be successful with some limitations. In Chapter 4, the effects of noise and nonlinearity introduced (separately) into the 5DOF system were also studied and the response surface metamodel proved to be robust to each of these, again with some limitations. An experimental cantilever beam is addressed in Chapter 5 to demonstrate the process of using simulation to "train" a response surface model. Then the model trained on simulation is applied to experimental data. Masses were placed at ten different locations on the beam. A response surface metamodel of the beam was constructed and with it the number and location of the masses on the beam were determined with some quantifiable degree of accuracy. Finally, Chapter 6 presents conclusions.

Chapter 2

BACKGROUND

2.1 Introduction

Before this thesis research is presented, background information on few different areas of research that relate to the use of metamodels (or response surface methods) in damage identification is reviewed. This review is not meant to be an exhaustive literature review. Rather, it presents a few different state of the art applications in each of the following three categories: Model reduction, damage identification and applications of response surface methods to structural dynamics problems. It also presents a brief review of response surface terminology.

2.2 Model Reduction

Because it has been emphasized that metamodels may be used with reduced data sets, a review of traditional model reduction methods follows so that the advantages and disadvantages of response surface metamodels may be seen. Model reduction methods have been used in conjunction with structural dynamics problems for many years.

Hemez and Masson provide a review of exisiting model reduction methods in their 2002 LANL Technical Memo, "Model Reduction Primer" [5]. In this paper the authors emphasize that there are two families of model reduction methods, direct reduction methods and component mode synthesis, or sub-structuring. Direct reduction methods involve reducing matrices to a subset of actual degrees of freedom in order to improve computational efficiency. Sub-structuring

methods, most commonly applied in larger systems, are integrated from numerous subsystems that are condensed at their interfaces. Sub-structuring allows individual components to be analyzed separately and may be implemented on problems of unlimited size, given current computational capabilities.

Direct condensation methods involve formulation of a transformation matrix, T, that preserves all the eigen-characteristics of the original system. For example if we start with

$$(K - \lambda M)\mathbf{y} = 0 \qquad\qquad (2.1)$$

$$T\mathbf{c} = \mathbf{y} \qquad\qquad (2.2)$$

where K is the stiffness and M is the mass of a dynamic system and λ and $\mathbf{y}$ are eigenvalues and eigenvectors of the system respectively, then we seek a transformation matrix T such that Eq. 2.2 is satisfied. The vector $\mathbf{c}$ is, according to Hemez and Masson, "a vector of generalized coordinates representing the contribution of each column of matrix T" [5]. Equation 2.2 may be substituted into Eq. 2.1 resulting in transformed mass and stiffness matrices. The goal of direct condensation methods is to preserve the character of the first few modes of a system. Methods of direct condensation differ only in their choice of T.

The method of sub-structuring is briefly summarized as follows [5]. A large system is broken down into sub-domains and interface degrees of freedom are defined. Then generalized coordinates and corresponding T matrices must be defined for each substructure, as well as the reduced (or transformed) mass and stiffness matrices. Then substructures must be assembled into the interface problem and the newly reduced eigen-problem solved. The final step is to transform back to physical degrees of freedom in each sub-domain. The reader is referred to Hemez and Masson for specific examples of each of these major types of model reduction methods. Examples of a few papers in the literature that discuss the use of these model reduction methods in structural dynamics problems follow.

A paper by Masson, *et al.* [6] discusses a modification of the Craig-Bampton (CB) method of model reduction so that a system modification may be made without completely re-evaluating

the reduced order model used. The problem with the existing CB technique is that if one wishes to conduct a parametric study of design variables, the model must either be reformulated, or the modeler must live with large inaccuracies that are incurred by using the nominal model. The technique introduced in this paper allows modelers to modify the nominal model based on an *a-priori* knowledge of the deisgn parameters and hence avoid re-formulating the model for an acceptable analysis.

Bobillot and Balmés [7] provide another example of structural response simulated using reduced order (direct condensation) models. The authors examine two fluid-structure interaction problems, that of oil in a viscoelastically damped oil pan and that of a cryogenic stage of the *Ariane-5* launcher with fluid. The problems are quadratic (nonlinear) eigenvalue problems. Fluid and structure are coupled in such a way that the *M* and *K* matrices are non-symmetric and high order. Three classical methods of solving these types of problems are reviewed. They are the inverse iteration method, the subspace method, and the Lanczos method. The method introduced by the authors is a modification of classical Ritz vectors, called the Ritz method with residue iterations. The original eigen-problem is projected on some new, reduced basis, *T*. Then errors on the force vector due to the use of this new basis are calculated. Displacement residuals are then calculated and a strain energy indicator evaluated using these. The basis is then updated using the displacement residuals until some error tolerance is met. The problem is then applied to the coupled fluid-structure interaction problem and as a result is generalized to a multiple field solver. The application of the solver is comparable to existing methods with respect to both accuracy and efficiency.

Burton, *et al*. [8] look at two different methods of model reduction for use in nonlinear model updating. The first method is to simply use an "exact for the linear case" model reduction and apply the resulting model to the nonlinear case with updating performed on the difference between simulated and measured time histories. The second method involves using the same reduced nonlinear model as in the first case, but with updating on the singular value decomposition of the simulated and measured responses. The authors apply both methods to a simple four degree of freedom simulated problem with a cubic nonlinearity and attempt to see damage (reduced stiffness in linear springs) in the system. Both methods are able to detect

damage in an equivalent linear system in almost all cases. For the nonlinear system, more initial information is required (3 sensors out of four possible) to identify the introduced damage. Sensitivity to initial condition (very sensitive) and measurement noise (insensitive to 10% signal to noise ratio) are examined.

2.3 Damage Identification

It is the purpose of this section to examine some work that demonstrates current methods of damage identification. Modal methods of damage detection are recognized as the most commonly used method of damage detection, and the reader is referred to the wide body of literature already in existence on this topic [9].

Brockman, *et al.* [10] look at an experimental 5 DOF system with different types of linear and nonlinear input parameters. Features are identified that characterize these input (or damage) parameters. Masses and spring stiffnesses are different. Linear changes are introduced by replacing two springs with two of lower stiffness. Nonlinear changes are introduced by placing bumpers between two of the masses, effectively resulting in a nonlinear stiffness increase for the spring at that position. A "loose" model is also used to introduce nonlinearity. Shaker excitation is used with a shaped random input. For linear changes differences in the natural frequencies were calculated. Mode four is found to be most sensitive to damage in spring one and two. Differences in mode shapes are also examined and modes one and two are most affected. Nonlinear changes are detected by examining the power spectra. Those sensors closest to the nonlinearity contain more high frequency content than the original system. Probability density functions (PDF) of signal magnitude are also examined, because nonlinear systems often deviate from normal (Gaussian) PDF distributions. The authors found that this indeed occurs at the location of the nonlinearity. Examination of FRFs did not yield much useful information.

Lee, Kim and Shin [11] use frequency response methods to identify damage in a plate structure. The authors argue that an advantage of FRF methods over the use of modal methods is that modal data is limited to information near resonance points. Their method is derived from dynamic plate equations, with the introduction of a damage influence matrix, which depends on mode shape curvatures and a damage distribution function. Knowing measured frequencies and

other plate properties (intact plate mode shapes and natural frequencies), they backsolve for the damage influence matrix. They apply the method to a simulation of a damaged plate and apply noise as well. They are able to show that their method is robust up to about 10% random noise. They find that measuring and exciting at multiple points works the best for their damage identification algorithm.

Robertson, *et al.* [2] demonstrate the use of neural networks to locate and predict velocity of impact of a projectile into a composite plate. While many of the advantages of using neural networks are similar to those of response surface methods (use of single number features, straight forward relationships between input and outputs), the reader will note that the number of training sets used to achieve acceptable results is very high. The authors compare the performance of three different types of networks, multi-layer perceptron network, radial basis network and support vector machines. For all networks, separate models are built for 1) location and 2) velocity of impact. A full factorial of finite element simulations is performed (all input parameters set at all possible levels); this involved running the simulation with impact at 10 different velocity levels, at 10 different *x* locations and at 10 different *y* locations, for a total of 1000 runs. The neural networks are all trained on 500 of these runs and tested on 250 (remaining 250 were used for validation if required) using features derived from the strain history at several different elements. All networks are able to locate the impact within the resolution of the elements used in the finite element analysis. Velocities are also predicted well.

The authors then train and test their networks on an experimental set-up, in which the plate is tapped in each of 49 locations (a 7x7 grid) and strain data is collected at the corners of the grid. This time, networks are trained on 28 to 40 experimental setups (depending on the network formulation chosen) using similar features. While the number of training sets is significantly reduced for this set of tests, results are not as good as those detailed above. After testing on 147 test setups, it is found that the multi-layer perceptron network performs better with the limited training set available. Finally they use their models that were trained on the experimental setup to locate where a projectile shot at the plate impacted. None of the networks perform well. They hypothesize that this is due to the high energy of this impact test and also due to damage induced in the plate by the projectile impact.

2.4 Response Surface Methods

Because the basis of the formulation of the metamodels in this research is provided by the statistical techniques of response surface analysis, a brief review of the philosophies and terminologies is provided below. For a more extensive explanation, the reader is referred to the many publications in existence on this topic. This review relies primarily on *Response Surface Methodology* by Myers and Montgomery [3] and the *Design-Expert* Software Users Manual by Stat-Ease [13].

Rutherford [12] notes that there are a few different types of experimental designs for computer analysis. The first type is the sampling approach. Monte Carlo methods, Latin Hypercube and importance sampling all fall into this category. These methods involve sampling parameters from distributions and then running computational analysis (or physical experiments) to find output features. He notes that these may involve many simulations, especially when the event of interest is one that is low probability. Response surface methods make up the second category, these include classical response surface methods (the focus of this thesis), reliability methods, and spatial methods. Advantages of response surface methods are that they all tend to reduce the number of computational/physical experiments necessary to explore the response space.

As stated in the introduction the primary utility of using design of experiments or response surface methods (RSM) is that it provides a way of rigorously choosing a few points in a design space to efficiently represent all possible points. Many different types of designs have been proposed in the literature, all are different with respect to which points are chosen for representation of the full factorial set (the set of outputs that correspond to the combination of all input parameters set at all possible levels). It is important to note that no design, unless it includes every possible point of interest (full factorial), will ever provide a perfect fit. All designs will impose certain constraints on the form of the model that can be fitted. In the case of polynomials, more points added to the model means that a higher order model may be fitted. One of the biggest limitations of response surface metamodels is "aliasing" or a mixing of higher order effects. Designs with only a few points may be used to fit higher order surfaces, but great care must be taken, because the higher order effects will be mixed, or aliased, with other effects,

resulting in an inability to distinguish what the "true" effect is. Because the focus of this thesis is not to discuss the mechanics of response surface design, the reader is referred to Meyers and Montgomery [3] for further details.

Let us first consider the form which a response surface model takes. A response surface is a functional mapping of several input parameters to a single output feature. In our case, it is of a polynomial form

$$z = Ax + By + Cxy + Dx^2 ... + \varepsilon \qquad (2.3)$$

where in this case, z is the output feature of interest and x and y are input parameters, and ε is the error term. $A, B, C, D, \ldots$ are regression coefficients, determined by the method of least squares. The number of input parameters may be unlimited; here only two are considered because visualization is easier. Order of the model is determined by the number of points used to "train" it. Typically model properties of interest are those that characterize model fit quality, contribution of an individual variable to total model variance, parameter aliasing properties (how much one parameter gets "mixed up" with other parameters), and model resolution. When performing response surface analysis, it is customary to use normalized or "coded" input parameter values. Also, if power transformations of the model output feature result in a better fit, they are commonly employed.

Consider the following example. We are interested in the maximum displacement, z of some displacement response. Impulse magnitude, x, and stiffness, y, of the system of interest are known to affect the maximum displacement. Impulse magnitude is examined at x=[5,10,15,20] N and stiffness is examined at y=[2000,3000,4000,5000] N/m. Knowing these levels of interest, we can generate maximum displacements that correspond to each pairing of impulse magnitude and stiffness (constituting the full factorial, or all inputs at all levels). With this information, we ask the question, what is the best model, in the form of equation (2.3), that predicts the maximum displacement, given known impulse magnitude and location? In this particular example, x and y are "input parameters," the values at which we examine x and y are "levels." The maximum displacement, z, is the "output feature." The full factorial design is (4 levels)$^{(2 \text{ factors})}$ = 16

12

simulations or experiments to generate the maximum displacements of interest. If we picked some subset of the possible values of *x* and *y*, then we would have a "fractional factorial" design. We may then generate a model with linear and/or higher order terms or "effects."

Commonly used models are usually some fraction of the full factorial design space and are therefore called "fractional-factorial models". When building models the number of input parameter levels of must be considered. If more input parameter levels are included in a model, then a higher order metamodel may be constructed. The more levels incorporated into a design, the larger the design will be for the same resolution of a design with fewer input parameter levels. The following list is a brief summary of each of the models used in this work.

2^k factorial design – This design is for any number of model inputs considered at two levels. These types of designs are useful in doing input parameter screening or determining how much each individual parameter contributes to the total model variance. Those that do not contribute much can be discarded. Larger "fractions" of the full factorial design will result in higher resolution designs with more design points.

Plackett Burman Design – A two level fractional factorial design (each input parameter set at two different levels). Because this design has a complex aliasing structure, it is commonly used for parameter screening purposes, or designs in which main effects (first order terms) are thought overshadow any higher order effects.

Central Composite Design – A design for input parameters with three to five levels. Often used to fit second order response surfaces. Runs consist of a center point, and then the corners of a square (or cube or higher order equivalent) and axial points, as in Figure 2.1. May be *rotatable* (error structure the same, no matter how the points are oriented) if axial points are chosen correctly.
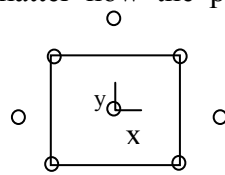
Figure 2.1: Qualitative design space for a two parameter central composite design. Circles are design points, *x* and *y* are input parameters.

Face Centered Cubic Design – A central composite design with axial points set at a normalized distance of one away from the center, as in Figure 2.2. Not necessarily rotatable.
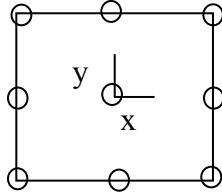
Figure 2.2: Qualitative design space for a two parameter face centered cubic design. Circles are design points, *x* and *y* are input parameters.

2.5 Application of Response Surface Methods to Structural Dynamics Problems

In addition to traditional model reduction methods, the application of response surface methods to structural dynamics problems has also been researched (though very little was found in the literature that was specific to the damage identification problem).

Huh and Haldar [14] define a hybrid method for considering the reliability of structures subject to short duration nonstationary dynamic loadings and perform damage prognosis of two theoretical structures. The authors consider a hybrid method, consisting of stochastic finite element modeling, response surface methodology and the first order reliability method. They focus on the formulation of three different types of response surface models relating structural material and geometry properties to probability of failure. The authors choose iterative combinations of second order polynomials (with and without interaction terms) and saturated and central composite designs in order to achieve efficiency and accuracy. Huh and Haldar provide examples of the use of these models on a two story steel frame structure (using El Centro time history) and on a 13 story steel frame structure (using Northridge time history). They suggest sensitivity analysis to further simplify large problems.

Gao, *et al.* [15] provide an example of the use of response surface methods in a mechanical setting. They examined design optimization and evaluation of a brushless DC spindle motor for better performance, quality, and decreased life cycle cost. The authors examine the use of a

mixed resolution rotatable central composite design. It is explained that using a CCD requires significantly less experiments (75) than a 3 level (2187) or a Taguchi design (225). For a mixed resolution CCD, defining relations are set up such that only factors that are important are examined on all levels. Control factors (whose higher order interactions might be important) and noise factors (whose higher order interactions are deemed unimportant) are defined. Defining relationships of the design are set up such that linear terms of all control and noise factors, quadratic terms of control factors, interactions between control factors and interactions between control and noise factors are estimated. Quadratic terms and interactions of noise factors are eliminated by making the axial points for the noise factors zero. Compared to a regular CCD, which would have 75 experiments required for their setup, their mixed resolution design requires only 41 experiments to estimate 30 model terms. Unlike Huh and Haldar [14], their method is not iterative, using only one model to relate input parameters and output features. They achieved promising results on their spindle motor example, which related geometric properties of the spindle to torque output.

Meckesheimer, *et al.* [16] concentrated on comparing different types of metamodels for use in discrete/continuous applications. While the authors do not apply their methods to damage identification problems, it is clear that some of the methods may be applied in this setting. For example a continuous-discrete formulation may be used in deciding if a structure is damaged (discrete) and then, if so, how much damage has been incurred. The authors examine linear regression models, radial basis functions, kriging models, and five types of designed experiments (full factorial, D-best latin hypercube, full factorial latin hypercube, hammersley sampling sequence, and uniform designs). They then look at combining these metamodels in different ways such that a combined discrete/continuous response is best estimated. Three different ways of estimating these combined responses are introduced. The first is the combined metamodel strategy (one metamodel for both continuous and discrete parts). The second is a metamodel plus the original logic (the discrete part is known *a priori*). The last is to have two different metamodels, one which estimates the continuous part and one that estimates the discrete, or logical part. Logical models (*e.g.,* neural networks) are suggested. Large errors at the discontinuity are likely to be encountered with all models. A case study of a desk lamp design is examined, metrics of model fit are studied, the mean square error, the mean absolute error and

the maximum absolute error. From the example, the authors conclude that the state-selecting metamodel used in combination with second-order polynomials is an accurate and efficient method.

Hemez, Wilson and Doebling [17] explore the use of design of experiments for model updating of a nonlinear impact problem. Model updating often involves solving an inverse problem; in this case, it may be formulated by asking the question, "Knowing what model responses are, what are the model inputs?" Use of models generated using design of experiments methods allowed the authors to optimize model parameters and thus determine what some of the experimental model input parameters were. Then once the values of these input parameters are known they are able to improve their higher fidelity finite element model. The authors use the correlation between test data and model predictions based on independent features (time of arrival and peak acceleration) as their objective function. The authors are successful in determining what some of these parameters are and are able to independently validate some of their parameter values.

Cundy, *et al.* [18] examine the use of response surface methods and Bayesian screening methods to perform parameter screening on a threaded assembly subject to transient excitation. The set of twelve input parameters involve dynamic and static coefficients of friction and preloads of threads in the assembly. Output features were temporal moments (successive integration of the acceleration time history times the time to successive powers; these are often used to describe transient dynamic signals). The authors use a two level Plackett Burman design to determine contributions of individual parameters to total model variance. They compare this to Bayesian screening methods. The Bayesian definition of probability accounts for subjective knowledge of the analyst, as opposed to the frequentist view of probability, which is based only on the number of occurrences of each event. Using Bayesian model screening, prior liklihoods are assigned to input parameters based on the analyst's knowledge of the problem. Then a form of Markov Chain Monte Carlo sampling called the Gibbs sampler (a single direction sampler) is used to sample models of unknown distributions. Models that fit the data well are visited more often, those that are a poor fit are visited less often. The analyst is then able to identify the model form which best captures the effects and output features of interest. Both of these methods are

compared to the more traditional general sensitivity analysis, which examines how much each output feature changes when each input parameter is changed one at a time (a simple, linear, finite differencing method). All methods resulted in the same six parameters screening out of the original set of twelve thought to be important.

Shinn, *et al.* [19] examine the estimation of error of a metamodel used in a nonlinear dynamics application. A single degree of freedom (SDOF) system is designed to model an impact test of an elastomeric (nonlinear) foam material. Two response features are identified. These were peak acceleration and time of arrival of this peak. Several different nonlinear models of the foam are created and for use in the context of the SDOF model with varying degrees of accuracy. In order to assess the predictive fidelity of the model, an error surface is fit. It is noted that the error surface cannot be fit just to model points; if this is done, the error surface may reflect zero everywhere, because error at model points is typically very small. The authors also state that the error surface must be bounded and that the bounds must account for all sources of model variability and uncertainty, whether they are analytical, experimental or numerical.

Chapter 3

LINEAR FIVE DEGREE OF FREEDOM SYSTEM

3.1 Introduction

A linear five degree of freedom (henceforth 5DOF) system was simulated in Matlab™ [20] and explored using response surface analysis. Because the focus of this thesis is the process of using response surface analysis in damage identification applications, the 5DOF system was deemed appropriate for analysis because of its simplicity. The methods examined were not only tested on a linear 5DOF damaged system, but also on one subject to noise and one with a nonlinearity introduced (addressed in Chapter 4).

Before delving into the analysis of the 5DOF system, it will be useful to first show the general steps of doing damage identification using RSM. Figure 3.1 shows, in flow chart form, the entire process. First the system of interest must be identified (Step 1 on the flow chart). Step 2 is of primary importance to the damage identification process; it is identification of input and output features. It will be shown how the choice of these can dramatically affect how well a metamodel generated using RSM is able to perform damage identification. In the case of dynamic structural systems, inputs must be controllable and are often those material and structural properties that may be changed or "damaged" (such as stiffness, mass and damping). Output features are usually single number scalars derived from time or frequency domain data. The appropriate choice of output features will be discussed more later.
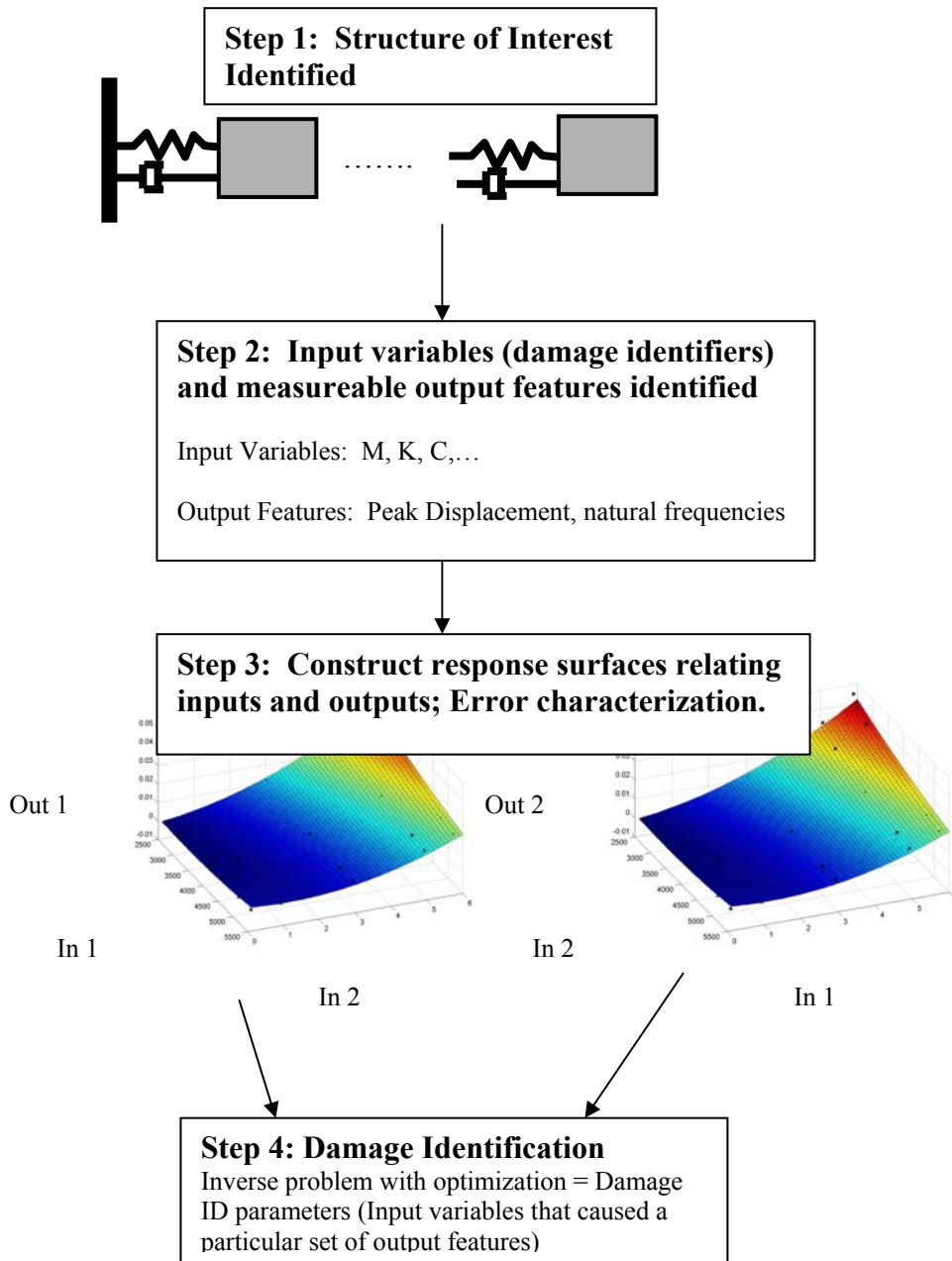
Figure 3.1 Four steps for doing damage identification using RSM.

The type of RSM is chosen next in Step 3. This choice will dictate the design points that must be simulated or experimentally derived. Then the mapping between inputs and outputs is defined by, in this case, a multiple-regression, least-squares algorithm resulting in a model that has a polynomial form. An important concept to note is that due to the functional form of this relationship, one model must be generated per output feature. For example, if the analyst wishes

to relate input variables to peak acceleration and time of arrival then two separate metamodels must be generated. Finally, after the model has been trained on the set of *design points* (known input variable and output feature pairs), it may be used in an inverse sense to do damage identification in Step 4. The question, "Knowing measured output features, what were the input parameters that lead to such values?" must be answered. Of course, in order to have some confidence in the answers derived, running extra points to characterize the error between the response surface metamodel and simulation and/or experiment is necessary. The following subsections of this chapter will be divided into the steps shown in Figure 3.1 for the case of the linear deterministically simulated system.

3.2 Step 1: Definition of Structure of Interest

As stated previously, the focus of this chapter is a simulated 5DOF system, consisting of springs, dampers and masses, connected as shown below in Figure 3.2. An impulse excitation is used. The simulation was coded into Matlab™ [20] by Dr. Gyuhae Park. Both time and frequency domain data were saved.
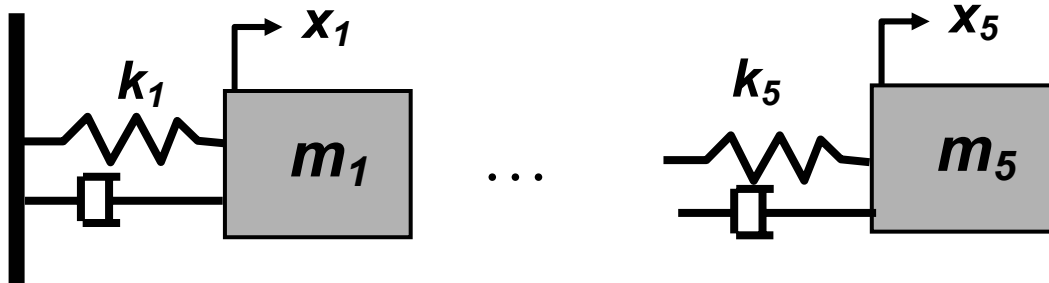
Figure 3.2 5DOF simulated system

Table 3.1: Input parameter identification for linear 5DOF system.

System Parameter	Value(s)
Spring Stiffness, k1-k5	2000-10000 N/m
Mass, m1-m5	2.0-10.0 kg
Damping, c1-c5	1.0 kg/s
Impulse Magnitude	0.1-5.0 N
Impulse Location	1, 2, 3, 4, 5 (unitless)

All system parameters and the range of their values are shown in Table 3.1. The only parameter held constant for the initial study was damping.

3.3 Step 2: Selection of Input Variables and Output Features

Input parameters chosen were stiffness and mass (each could have five different values, but all five locations were the same), as well as impulse magnitude and impulse location. While frequency domain features were eventually used for the damage identification problem, in this case, the output features chosen were derived from the displacement time history. Time series features are of interest for eventual application in nonlinear problems, where frequency domain features may be more difficult to extract.

This thesis makes extensive use of temporal moments, a concept first introduced for use with transient dynamics problems by Smallwood [21]. Temporal moments are useful in metamodeling because they are single number characterizations of time series data and usually at least one of the first few is able to discriminate between damage states. A general equation for taking the ith temporal moment, M_i of a function $f(t)$ about time $t=0$ is

$$M_i = \int_{-\infty}^{\infty} t^i f(t)^2 \, dt \qquad (3.1)$$

where $f(t)$ is the time series of interest.

Hemez and Doebling [22] have recently explained the physical interpretation of moments M_0 through M_2. Normalized, or central moments are called E, T, and D (where all moments are normalized by the zero order moment). E is the energy of the signal. T is the centroid of the signal or the time at which half of the energy has arrived and half has yet to come. D is the root mean square duration of the signal and may be thought of as equivalent to standard deviation. Hemez and Doebling note that usually "the significant part of the transient's energy should be within 2 or 3 RMS durations around the centroid T." In the same paper, Hemez and Doebling also show that temporal moments may be transformed back to time series with the same statistical properties as that from which they were generated. This implies that much valuable

information about the signal is retained in the use of these features. Other moments are used in the literature, but are not addressed in this work, because as the order of the moment increases, physical interpretation becomes more difficult.

In this investigation of response surface performance, the first moment, E, from the displacement time history at Location 3 was used as a feature, chosen arbitrarily among the choice of five possible locations. Only one location was used for moment calculations because it was desired to show that response surface methods may also be used as reduced order models. That is, much information about a system may be gained from a small number of measurement points.

Another feature examined is related to the rate of decay of the displacement time history. This seemed a logical output feature to use, given that the problem is one of free vibration after the impulse, and displacement time histories typically look like Figure 3.3. Such a feature is well known in vibration literature as the *log decrement*, δ [23],

$$\partial = \text{Ln}\left[\frac{(\exp[-\zeta\omega_n t]\sin[\omega_d t + \phi])}{(\exp[-\zeta\omega_n(t+T)]\sin[\omega_d(t+T)+\phi])}\right] \qquad (3.2)$$

where *t* is time, *T* is period, ω_n is natural frequency, ω_d is damped natural frequency, ς is damping ratio, and φ is phase angle. It can be seen that the log decrement depends not only on damping, in the form of ω_d (which is not changed in this simulation), but also on stiffness and mass (in the form of ω_n). For the 5DOF system, a log decrement parameter may be empirically fit using the following form

$$f(t) = e^{at+b} \qquad (3.3)$$

where *f(t)* are the positive peaks of the displacement time history, *t* is time and *a* and *b* are constants defining the curve. This curve is shown in red on Figure 3.3. The fit curve was then integrated analytically

$$\int e^{at+b}\, dt = \frac{e^{at+b}}{a} \qquad (3.4)$$

where *a* and *b* are as above. The resulting area was used as a feature (again, displacement time history from Location 3 was used), and called the "log decrement feature" or "LD." This new feature is also sensitive to the amplitude of the vibration as well.
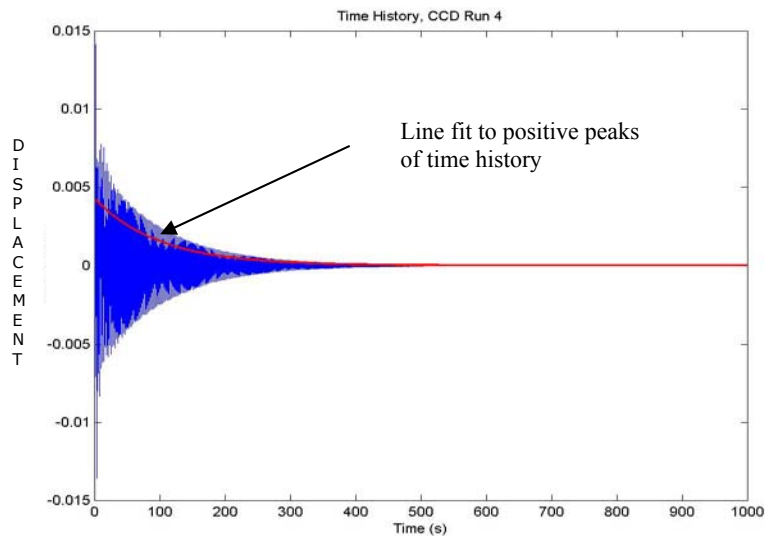
Figure 3.3 Typical displacement history and line fit to the positive peaks.

While the analyst can make educated guesses as to which features will be appropriate for use in a damage identification problem, it should be noted that choosing features is often an iterative process. An initial set is chosen, models fit, and the damage identification problem attempted. If the results are non-unique, often the analyst must choose new features which yield unique results for the damage identification problem. This problem will be discussed in greater depth in the section on Step 4.

3.3.1 Variable Screening

In order to determine if the output features chosen were indeed sensitive to some or all of the potential input parameters (mass, stiffness, impulse magnitude, impulse location), preliminary variable screening was conducted before response surface models were built. It is important to realize that while variable screening may not be the most important step in a small problem such as the 5DOF system, in large problems with many potential input parameters, variable screening can be well worth the time spent on it. An example is the Los Alamos Threaded Assembly

problem [18], in which 12 potential input parameters were screened down to a subset of 6 that were actually important to the chosen output features. Variable screening can significantly reduce the number of runs required to generate an adequate response surface model.

For the 5DOF system, two types of screening (General Sensitivity Analysis and Significant Effects Screening) were conducted and corroboration between the two methods sought. Both methods screened for only linear input parameter effects (also referred to as *main effects*). No higher order effects were considered. The input parameters of interest were mass, stiffness, impulse magnitude and impulse location. The sensitivity of the two output features, E (first moment) and LD (the empirical "log-dec" feature) to those input parameters was sought. If the output features were found to be insensitive to any of the parameters, those parameters were considered for removal from the response surface design.

3.3.1.1 GENERAL SENSITIVITY ANALYSIS

General Sensitivity Analysis (GSA) is typically conducted by analysts as a fast way to tell which input parameters are important to a particular output feature. A first order derivative of the output feature of interest with respect to each input parameter is computed using finite differencing. The value of this derivative is computed with the level of the input parameter under consideration set at its extreme values, while the values of the remaining input parameters are held at their nominal values.

Table 3.2 GSA input parameter values and corresponding output feature values.

	Input Parameters (specified)				Output Features (calculated in Matlab)	
	Imp (N)	Stiff (N/m)	Mass (kg)	Loc	LD (m*s)	E (m^2*s)
I hi	5	6000	6	3	2.4509	0.0138
I lo	1	6000	6	3	0.4902	0.0006
S hi	3	10000	6	3	1.0112	0.0030
S lo	3	2000	6	3	2.8194	0.0149
M hi	3	6000	10	3	1.9916	0.0050
M lo	3	6000	2	3	0.5093	0.0048
L hi	3	6000	6	5	1.9232	0.0085
L lo	3	6000	6	1	1.0505	0.0026

For the 5DOF system, mass, stiffness, impulse magnitude and impulse location were considered input parameters. The set of simulations run are shown in Table 3.2. For brevity, input parameters have been abbreviated in tables and figures as Impulse Magnitude (I), Stiffness (S), Mass (M), and Impulse Location (L). Each input parameter is set at its low range value and then its high range value while the others are held at their middle, or nominal value. Output feature values were calculated using the 5DOF Matlab™ simulation. Estimates of the derivatives were then calculated using these input-output pairs according to the simple finite differencing formula

$$\frac{\partial \text{Out}}{\partial \text{In}} \approx \frac{\text{Out}_{\text{Hi}} - \text{Out}_{\text{Low}}}{\text{In}_{\text{Hi}} - \text{In}_{\text{Low}}} \qquad (3.5)$$

where *Out* and *In* refer to output features and input parameters (all normalized before the calculation to eliminate scaling issues), respectively, and *Hi* and *Low* refer to the level at which the input parameter of interest is set. Results of these finite difference calculations are shown below in Figure 3.4.
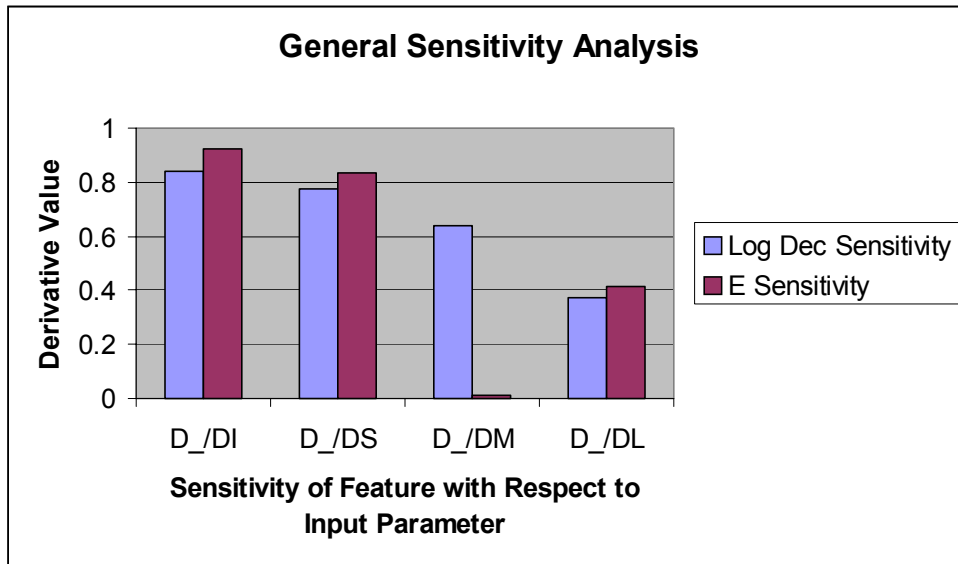
Figure 3.4 Results of general sensitivity analysis.

As can be seen in Figure 3.4, all input parameters were "important" to the LD feature, meaning that changing any of the input parameters while the others were held at their nominal values

resulted in a significant change in the value of the LD feature. It can also be seen that mass has very little effect on the E output feature. Hence the method has "screened out" the mass parameter, meaning that a future metamodel design relating the input parameters and the E feature could be based on only the three inputs significantly influence E. The fourth parameter, mass, found to not influence the E feature, could be kept constant and equal to its nominal value, or Mass=6 kg.

3.3.1.2 SIGNIFICANT EFFECTS VARIABLE SCREENING

Another method of variable screening implemented was significant effects variable screening or linear variable screening. A particular input parameter's contribution (linear effects only) to the total model variance was analyzed. The method of significant effects is an analysis of variance method and is expressed as follows

$$
\begin{aligned}
SS_i &= \frac{n}{4(Out_{Hi} - Out_{Low})^2} \\
PC &= \frac{SS_i}{\sum SS_i}
\end{aligned}
\qquad (3.6)
$$

where SS_i is the sum of squares for a particular input parameter, n is the number of terms in the designed experiment used (in this case, 12, because a Plackett Burman Design was used, see Chapter 1 for more details on this two level design), Out is the output feature of interest, and Low and Hi are the input variable levels. PC is the percent contribution of a particular variable. Significant effects method provides an advantage over GSA because it is a probabilistic assessment of variable importance which is obtained through the analysis of variance (ANOVA).

In order to obtain the percent contribution, a two level factorial design must be used. As mentioned above, a Plackett Burman design was chosen because it is typically used for screening purposes. The choice of design dictates at what levels the input parameters are set; in this case various combinations of their high and low values for a total of twelve design points. To ensure that false positives were not obtained two "dummy" input parameters (or "dummy variables") were introduced, to ensure that they were determined to bet as unimportant. Output features

corresponding to the designed input parameters are then calculated using the Matlab™ 5DOF simulation.   The percent contribution may be calculated using the Design Expert™ software. The results are shown in Figure 3.5 below.

E-Time, Significant Effects Screening

Log Dec Parameter, Significant Effects Screening
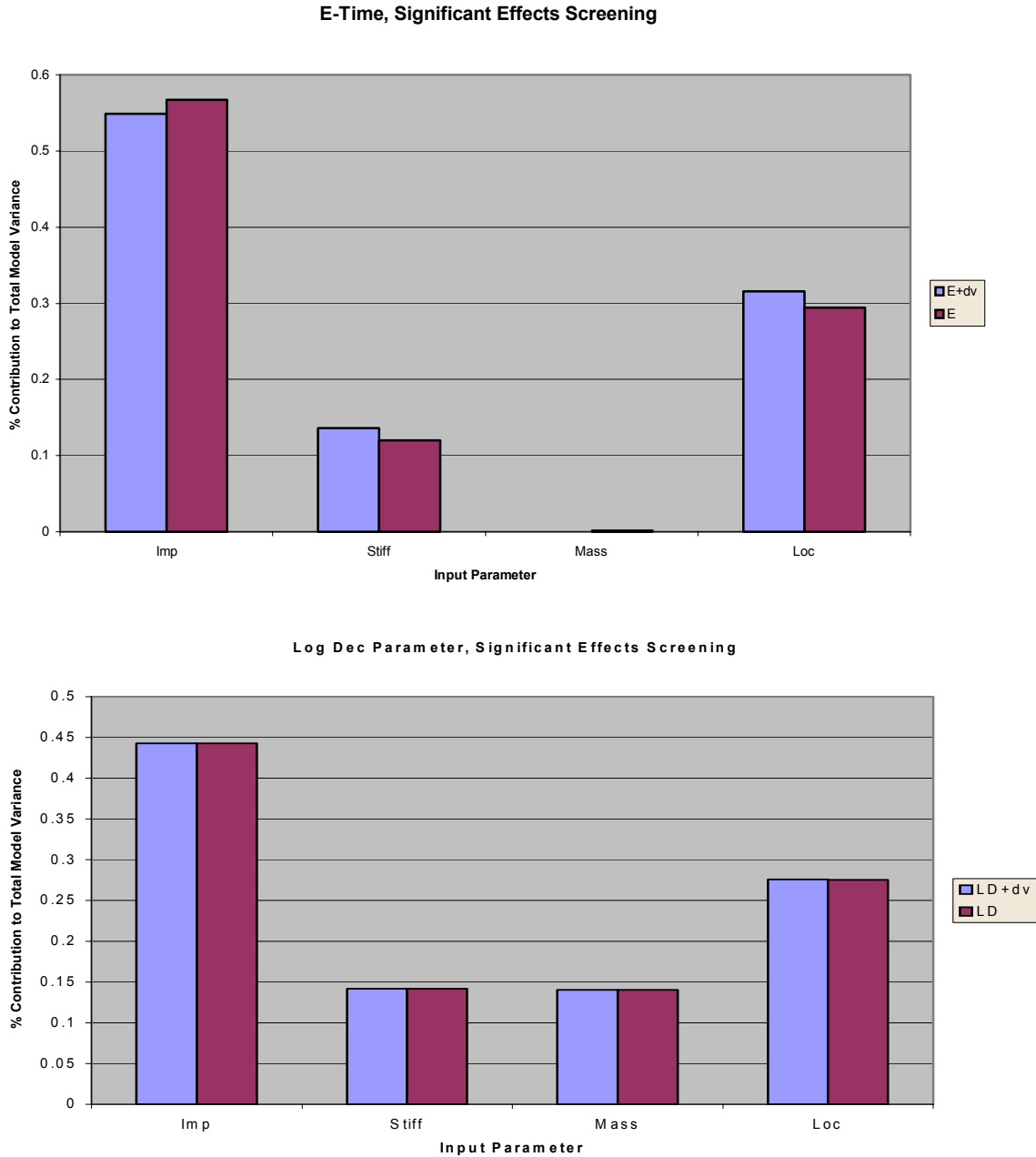
Figure 3.5 Significant effects screening results. "+dv" indicates the addition of dummy variables to the screening model.

Resulting percent contributions for screening with and without the dummy variables were very close and in some cases identical for input parameters of interest. In both the case of the LD feature and the E feature, the dummy variables were screened out (note that dummy input parameters were screened out with near zero percent contribution, which is why they are not shown explicitly on the plots). Again it was noted that all input parameters were important to the LD feature and mass was screened out of designs with E-time as the output feature.

3.3.1.3 VARIABLE SCREENING CONCLUSIONS

Results from variable screening suggest the following set-ups for higher order designs: For E models, the three input parameters, stiffness, impulse magnitude, and impulse location may be used. Mass screened out as un-important to the E feature with both of the screening methods tried. For models of the LD feature, all four input parameters could be used, as all of them were found to be important.

3.4 Step 3: Construction of Response Surfaces and Error Characterization

Several different response surface metamodels of the 5DOF system were designed using the results from the above variable screening process and the output features chosen. Types of models and output features used were varied. Table 3.3 shows the models designed. The first column designates which of the input parameters were chosen for the design and how many levels were considered. The number of full factorial runs was calculated as (Number of Input Parameter Levels)$^{\text{Number of Input Parameters}}$ for comparison purposes. A design with two input parameters at five levels each would have 25 simulations in the full factorial set. The number of input parameter levels and which points are chosen differentiate one response surface model from another (some of those listed under "model type" are discussed in Chapter 2, for details on all of those listed see Meyers and Montgomery [3]). Again, recall that the advantage of using response surface analysis is the ability to intelligently choose only a few of the full factorial set to construct an input-output relationship. All models were constructed with the aid of Stat Ease Design Expert™ software [13].

Points used in designed experiments are chosen to maximize information over a minimum number of design points. A typical designed experiment is shown below. Input parameter levels

are dictated by the type of design chosen, in this case a central composite design. The 5DOF Matlab™ simulation is then run to generate the output features, in this case, the first moment or E feature. Mass and impulse location were kept constant with values of 7 kg and 3, respectively.

Table 3.3: Models of the 5 DOF simulated system.

Input Parameters (number of levels considered)	Number of Design Points	Full Factorial	Model Type	Output Feature Modeled
Stiffness (5), Impulse Magnitude (5)	9	$5^2=25$	Central Composite Design	E-Time
Stiffness (5), Impulse Magnitude (5)	9	$5^2=25$	Central Composite Design	Log Dec
Stiffness (5), Impulse Magnitude (5)	9	$5^2=25$	Taguchi	E-Time
Stiffness (5), Impulse Magnitude (5)	9	$5^2=25$	D-Optimal	E-Time
Stiffness (3), Impulse Magnitude (3)	9	$3^2=9$	3 Level Factorial	E-Time

Table 3.4 CCD design points for simulation of the E feature.
The design has two input parameters, each with five levels.

	Input Parameters		Output Feature
Design Point Number	Stiffness (N/m)	Impulse Magnitude (N)	E (m^2*sec)
1	3000.00	1.00	0.00110583
2	5000.00	1.00	0.00066356
3	3000.00	5.00	0.0276458
4	5000.00	5.00	0.016589
5	2585.79	3.00	0.0123797
6	5414.21	3.00	0.00550603
7	4000.00	0.17	2.39096E-005
8	4000.00	5.83	0.0281197
9	4000.00	3.00	0.00744588

The Design Expert software is then used to conduct multiple regression on the set of input-output pairs given above. The output feature may be subject to a power transformation (e.g. square root, log, ln, etc) in order to improve goodness of fit. For the above CCD, the resulting model had the polynomial form shown in tabular form for convenience. In this equation, the input parameters stiffness and impulse magnitude are normalized between the values –1 and +1, hence the coefficients in the model give an idea of the relative importance of each of the terms. This polynomial may be plotted (in actual units) as the response surface shown in Figure 3.6.

E-Time=

+7.446E-003	
-2.652E-003	*Stiffness*
+0.010	*ImpulseMag*
+7.469E-004	*Stiffness^2*
+3.311E-003	*ImpulseMag^2*
-2.654E-003	*Stiffness * ImpulseMag*
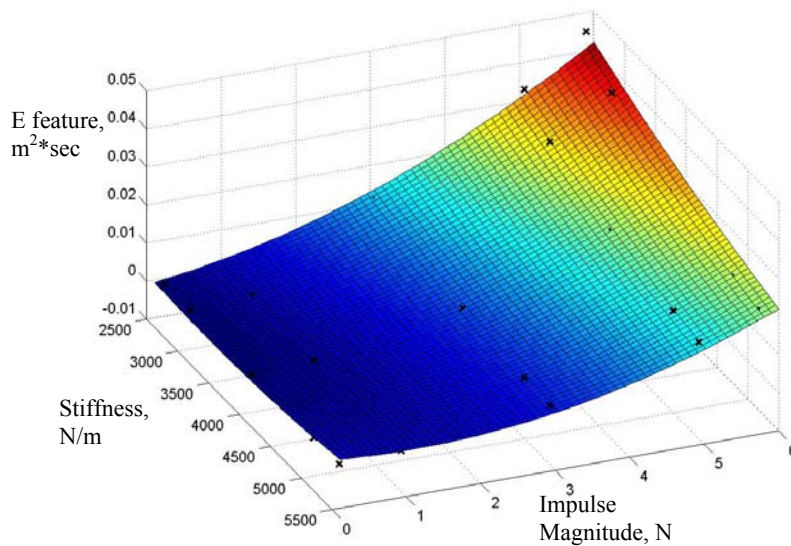
Figure 3.6 Response surface fit to CCD design points. X's denote the points designated as the "full factorial set."

Because the surface is an empirical relationship between inputs and outputs, it does not perfectly fit the design points. Appendix A discusses different types of error metrics that may be used to aid in deciding which design to choose and shows the results of calculating these metrics for the

designs in Table A1. In the case of the 5DOF system, it turned out that all response surface models generated were comparable, with very good error statistics. A central composite design was chosen because these are perhaps the most commonly used response surface models[3].

3.5 Step 4: Damage Identification

Before trying the damage identification problem, identification of system parameters with no damage was first attempted. This was done so that the mechanics of solving the inverse problem could be studied before attempting the damage identification problem.

As stated before, the primary purpose of the models generated in Steps 1 through 3 was to explore the different properties of response surface models. Following is a description of how the damage identification problem, or the inverse problem, may be solved. It was discovered that time series features originally chosen were inappropriate for doing damage identification and the problem had to be reformulated with frequency domain features. Both models will be discussed, and reasons for success of the second model explained. Reformulation of models is often necessary, because the ability to solve the inverse problem is highly dependent on output features chosen. Hence, building models and trying the inverse, or damage identification, problem may be an iterative process, ending when the inverse problem is successfully solved.

3.5.1 Step 4a: Attempts to Solve the Inverse Problem Using Time Series Features

In order to investigate the mechanics of the inverse problem, central composite designs with four input parameters, mass, stiffness, impulse magnitude and impulse location, were constructed. Reviewing the previous steps, Design Expert™ was used to choose the design points, the Matlab™ simulation was then run with the input parameters at the chosen levels and corresponding output features derived. Finally Design Expert™ was used to generate the response surface that relates input parameters to output features. Now the answer to the following question was sought "Can input parameter values (damaged or undamaged) be inferred from measured output features?" In Step 4a, this problem was first attempted using time series features, which resulted in an ill-conditioned inverse problem, that is, one without unique solutions. The following paragraphs are a brief summary of these results, for more detail please refer to Appendix B.

At first, no "damage" was introduced; the inverse problem was solved to see if input variables that caused a particular output feature could be found and the actual mechanics of the inverse problem understood.   Recall, that the output features initially chosen for these models were the time series features, E and LD at Location 3. Because solving the problem did not initially work using just Location 3, E and LD were chosen from Location 5 as well. Additionally, it was assumed that three of the inputs were known, and the fourth (stiffness) was solved for. A simple error minimization scheme was implemented using MatLab™'s *fminsearch* routine.   The objective function was an error minimization between actual and predicted feature values. A random start point was used for each optimization, and optimizations stopped once a minimum was achieved.   However, these minima proved to be non-unique, with many equally valid solutions, which should not be a surprise, because solutions to inverse problems are often non-unique due to their non-functional form.

For this reason, correlation between output features was examined.   The more uncorrelated output features are, the more linearly independent information they provide about the system. It was discovered that E and LD features at all sensors were highly correlated (correlation coefficients near 1),

$$\rho_{xy} = \begin{bmatrix} 1.00 & 0.91 & 1.00 & 0.91 \\ 0.91 & 1.00 & 0.91 & 1.00 \\ 1.00 & 0.91 & 1.00 & 0.91 \\ 0.91 & 1.00 & 0.91 & 1.00 \end{bmatrix} \qquad (3.7)$$

where ρ_{xy} is the matrix of correlation coefficients, and the order across and down is E3, LD3, E5, LD5. Highly correlated features mean that no new information is gained by using more than one of them. New, uncorrelated output features were sought. The next logical ones to try were the natural frequencies of the system. As shown in the next section, they are not highly correlated. For this reason, the problem was reformulated and solved using natural frequencies as output features.

3.5.2 Step 4b: Damage Identification of the 5DOF System with a Reformulated Metamodel

Again, iteration through the previous three steps is necessary. Specific details will be neglected. Step 1 is to identify the system (again the 5DOF system). Step 2 is to choose model inputs and outputs, detailed in the paragraph below. Step 3 is to design and run the necessary experiments to generate the relationship between the input parameters of interest, in this case stiffness and location, and measureable output features (natural frequencies).

In addition to changing the output features, the response surface model inputs were changed to better reflect the purpose of the damage identification problem, identification of damage magnitude and location. Input parameters were stiffness (varied from 2000 to 6000 N/m) and location of damaged spring (1 to 5). A stiffness of 6000 N/m was designated "healthy" and was included in the model so that the "healthy" system might also be identified. Mass and damping were held constant at 7 kg and 1kg/s, respectively. All five stiffnesses were set to a nominal, or "healthy" value of 6000 N/m and then damage could be introduced by changing a stiffness at one of the five locations to a lower value (2000, 3000, 4000, or 5000 N/m). With two input parameters each with five possible levels, the full factorial case would be 25 simulations. Impulse magnitude was 5 N at Location 3.

As stated previously, the response features were the values of the five natural frequencies, with Location 3 as the input measurement location and Location 5 as the output measurement location. Frequency domain features may be easily used in this simple linear simulation, but may not be so easily used in the presence of nonlinearities. This issue will be addressed in the Chapter 4.

A model was built using a face centered cubic (FCC) design, requiring nine Matlab™ simulations to determine what the natural frequency values, ω_n, were corresponding to the design points. An FCC design is simply a central composite design with its axial points set at +/-1 (coded value) away from the center point (see Chapter 1 describing different types of designs). The face centered cubic design used is shown below in Table 3.5, and the polynomials generated for each frequency are shown in Table 3.6. Below, in Figure 3.7, is an example of one of the

response surfaces generated, shown as a contour plot (taken from Design Expert™ software [13]
used to generate the models). The dots are the model design points shown in Table 3.5.

Table 3.5 FCC design used for damage identification of the 5DOF system.

Design Point	Input Parameters		Output Features				
	Stiffness (N/m)	Location	ω_1 (Hz)	ω_2 (Hz)	ω_3 (Hz)	ω_4 (Hz)	ω_5 (Hz)
1	2000	1	6.25	20.75	35.50	47.75	55.75
2	6000	1	8.25	24.25	38.25	49.75	56.25
3	2000	5	8.00	19.25	31.75	45.75	55.25
4	6000	5	8.25	24.25	38.25	49.25	56.25
5	2000	3	7.00	22.5	32.5	48.25	51.50
6	6000	3	8.25	24.25	38.25	49.25	56.25
7	4000	1	7.75	22.75	37.00	48.50	56.00
8	4000	5	8.25	23.00	35.25	47.00	55.50
9	4000	3	8.00	23.75	36.00	49.00	53.25
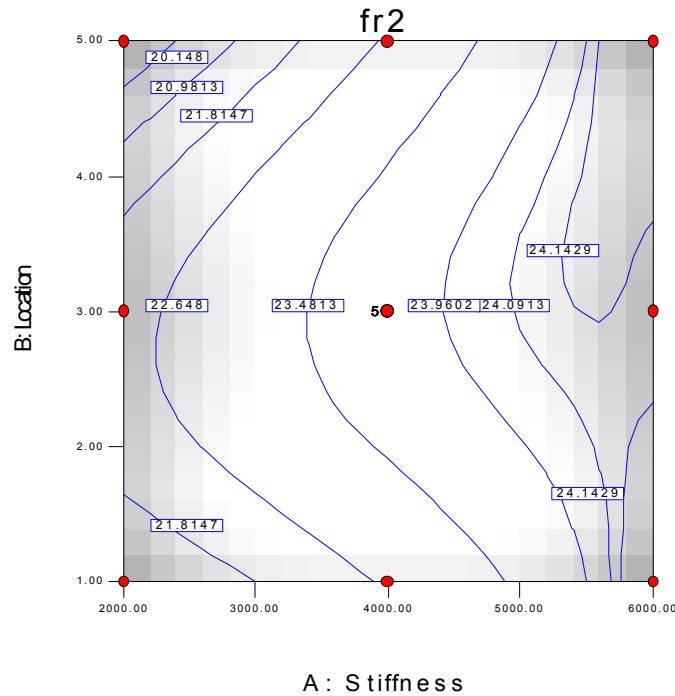
Figure 3.7 One of the five response surfaces generated for the damage identification problem.
Model input parameters are stiffness and location, output in this plot is the second natural
frequency.

Table 3.6 Summary of polynomials generated; units of stiffness and location are scaled between −1 and +1.

Frequency	Equation (S=Stiffness, L=Location)
$(\omega_1)^{-1.6} =$	0.036 - 5.137E-003*S - 1.798E-003 * L + 3.412E-003 *S^2 + 7.229E-005*L^2 + 4.347E-003*S*L -2.549E-003*S^2* L - 7.152E-005*S*L^2
$\omega_2 =$	23.80 + 0.87*S - 0.56*S^2 - 1.06*L^2 + 0.38*S*L - 0.38*S^2*L + 1.25*S*L^2
$\omega_3 =$	35.94 + 2.87*S - 0.92*L - 0.41*S^2 + 0.34*L^2 + 0.94*S*L - 0.56*S*L^2
$\omega_4 =$	48.93 + 0.50*S - 0.58*L - 1.01*L^2 + 0.50*S*L + 0.75*S*L^2
$\omega_5 =$	53.32 + 2.37*S - 0.17*L + 0.38*S^2 + 2.26*L^2 - 2.00*S*L^2

Once the relationship between the input parameters and each of the five output features have been established, Step 4 is completed by optimization using the resulting response surfaces in order to do damage identification. That is, knowing the natural frequency values, can the magnitude and location of the reduced stiffness be found? Because natural frequencies were used and they are not highly correlated, optimization works better than with the time series features used in the previous section. The matrix of correlation coefficients (ρ_{xy}) of the five natural frequencies is, where the order across and down is $\omega_1, \omega_2, \omega_3, \omega_4,$ and $\omega_5.$

$$\rho_{xy} = \begin{bmatrix} 1.00 & 0.32 & 0.44 & 0.43 & 0.34 \\ 0.32 & 1.00 & 0.47 & 0.46 & 0.32 \\ 0.44 & 0.47 & 1.00 & 0.34 & 0.44 \\ 0.43 & 0.46 & 0.34 & 1.00 & 0.34 \\ 0.34 & 0.32 & 0.44 & 0.34 & 1.00 \end{bmatrix} \qquad (3.8)$$

The optimization procedure used for this set of models was a Nelder-Meade simplex routine embedded in the Stat Ease Design Expert™ software [13]. It also incorporates the desirability function of Myers and Montgomery [3] which is as follows

$$d = \left(\frac{y-A}{B-A}\right)^s, A \le y \le B$$

$$d = \left(\frac{y-C}{B-C}\right)^t, B \le y \le C$$

(3.9)

The powers s and t weight how quickly the function travels to a maximum desirability of 1 at target value B, from the range endpoints of either A or C. Desirability is a criterion placed on the measured output values provided. The optimizer then changes the value of the input parameters sought until maximum desirability is achieved near the target output feature values provided. Results are then ranked in order of decreasing desirability. In all cases, the standard followed was to choose the set of input parameters that resulted in the highest desirability rating on the output features.

To test how well the optimization procedure worked, the full factorial set of experiments was optimized (this includes the 9 design points plus 16 points not included in the design, for a total of 25 points). That is, knowing the five natural frequency values, could the change in stiffness (if any) and the location of the change be identified? The damage identification matrix is shown in Table 3.7 below, with stiffness and location to be determined by the optimization routine (actual values of stiffness and location are given in Table 3.7). Frequency values were derived from the MatLab™ simulation.

Table 3.7 Full factorial set of damage identification runs. Design points are shown in bold.

	Input Parameters (To be determined)		Output Features (Known, simulated or measured)				
Factorial Point	Stiffness (N/m)	Location	ω1 (Hz)	ω2 (Hz)	ω3 (Hz)	ω4 (Hz)	ω5 (Hz)
1	**2000**	**1**	**6.25**	**20.75**	**35.50**	**47.75**	**55.75**
2	3000	1	7.00	22.00	36.25	48.25	55.75
3	**4000**	**1**	**7.75**	**22.75**	**37.00**	**48.50**	**56.00**
4	5000	1	8.00	23.75	37.75	48.75	56.00
5	**6000**	**1**	**8.25**	**24.25**	**38.25**	**49.25**	**56.25**
6	2000	2	6.50	23.75	34.25	42.75	54.25
7	3000	2	7.25	24.00	36.00	44.25	54.50
8	4000	2	7.75	24.25	37.25	45.75	55.00
9	5000	2	8.00	24.25	38.00	47.75	55.50

10	6000	2	8.25	24.25	38.25	49.25	56.25
11	**2000**	**3**	**7.00**	**22.25**	**32.50**	**48.25**	**51.50**
12	3000	3	7.50	23.00	34.25	48.50	52.25
13	**4000**	**3**	**8.00**	**23.75**	**36.00**	**49.00**	**53.25**
14	5000	3	8.25	24.00	37.25	49.00	54.50
15	**6000**	**3**	**8.25**	**24.25**	**38.25**	**49.25**	**56.25**
16	2000	4	7.50	19.00	37.50	43.75	53.25
17	3000	4	8.00	21.00	38.00	45.25	53.50
18	4000	4	8.00	22.50	38.00	47.00	54.00
19	5000	4	8.25	23.50	38.25	48.25	55.00
20	6000	4	8.25	24.25	38.25	49.25	56.25
21	**2000**	**5**	**8.00**	**19.25**	**31.75**	**45.75**	**55.25**
22	3000	5	8.25	21.50	33.50	46.25	55.25
23	**4000**	**5**	**8.25**	**23.00**	**35.25**	**47.00**	**55.50**
24	5000	5	8.25	23.75	37.00	48.00	55.75
25	**6000**	**5**	**8.25**	**24.25**	**38.25**	**49.25**	**56.25**

Results are shown below in Figure 3.8 in the form of two plots of actual stiffness or location versus predicted stiffness or location. Ideally these results would plot on a line at 45˚ on the plot.
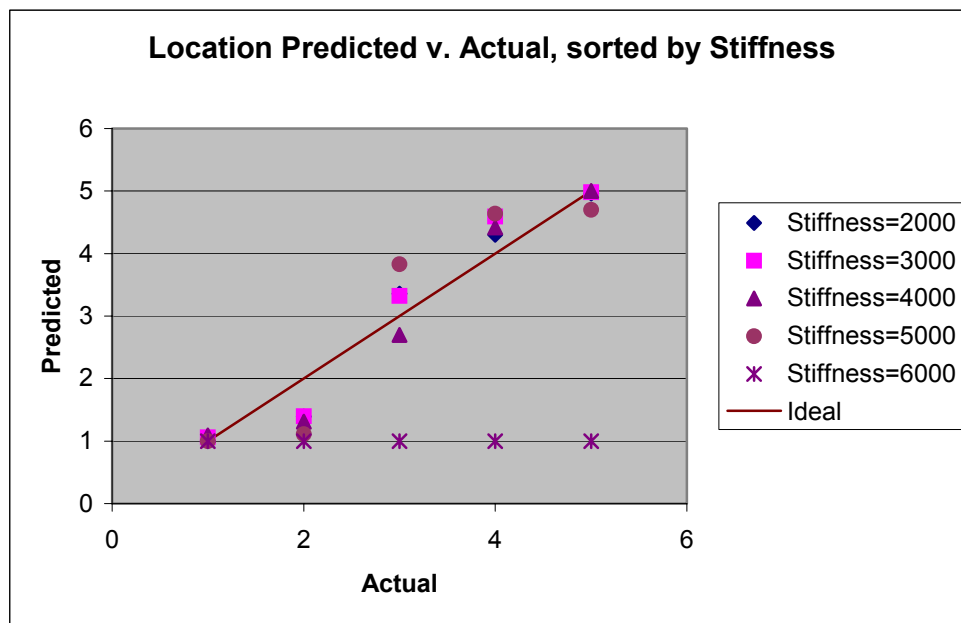
Figure 3.8 Location results of solving the damage identification problem using optimization.
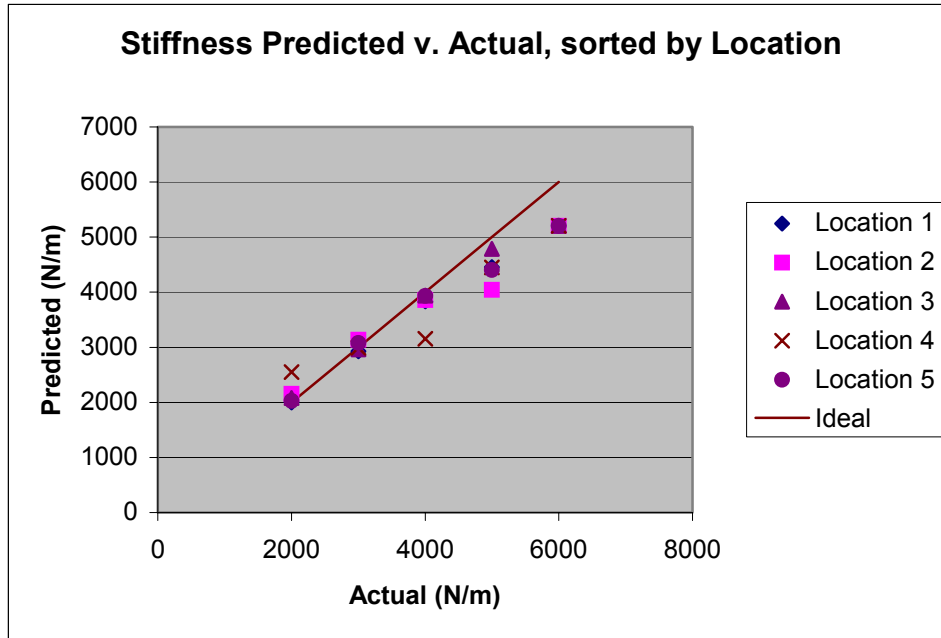
Figure 3.9 Stiffness results of solving the damage identification problem using optimization.

Note that all of the mis-identified "Location 1" values corresponded to the "healthy system" (all stiffnesses at 6000 N/m; these runs were included to see if the healthy system could be identified). It can be observed from Figure 3.8 that stiffness predictions drift below the ideal line as the stiffness increases. In fact all healthy stiffnesses came back with a value of 5206, Location 1. If the analyst can be expected to recognize a stiffness prediction of 5206 N/m at Location 1 as a "healthy" system, then the damage identification of this system is successful.

If the healthy system is not considered, due to its high location error, most of the errors on stiffness prediction are under 20% as can be seen in Figure 3.9. Higher error was expected at the stiffnesses (3000, 5000) and locations (2, 4) that were not included in the training data set and this was observed.

38

Relative Error on Predictions
(Healthy system predictions not included)
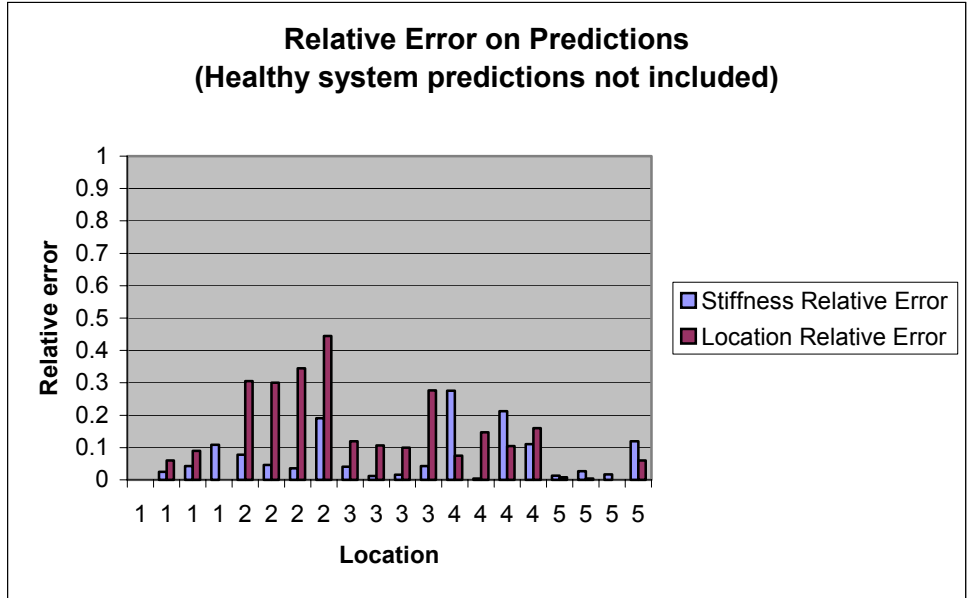
Figure 3.10 Relative errors of predictions for stiffness (increasing for each location) and location.

3.6 Conclusions

A response surface model was constructed of a 5DOF system, using data taken at only two of the five possible locations. The importance of choice of output features to the solution of the damage identification problem was demonstrated and it was shown that the more uncorrelated the output features are, the more linearly independent information they provide about a system. Natural frequencies were found to be acceptable output features to use (because they were uncorrelated). Using these features the magnitude of the damage (altered stiffness) was correctly identified for nearly 80% of the simulations tested. Stiffness reduction identification was accomplished by solving the inverse problem using a set of five polynomials, which were trained on nine of 25 possible data sets. Identification of the location of the damaged stiffness was somewhat less successful. One possible reason for higher location error might be because continuous input variables were used to represent discrete locations. The results of the linear 5DOF damage identification problem clearly demonstrate the potential of using response surface metamodels in their inverse formulation for damage identification.

Chapter 4

ROBUSTNESS OF THE FIVE DEGREE OF FREEDOM SYSTEM SUBJECT TO NOISE AND NONLINEARITY

4.1 Introduction

In order to determine how robust the response surface models and damage identification method of the previous chapter were, simulated "noise" was introduced into the natural frequencies in an attempt to mimic experimental variability. The response surface models trained on the deterministic, or "no noise" simulation were then used for identification of damaged springs. The response surface model proved to be robust to 3% noise introduced on the natural frequencies with some limitations.

The ability of response surface models to handle nonlinearities was tested with the introduction of a nonlinear spring (with no noise). A new response surface model was developed that could distinguish between a linear and a nonlinear system. In this setup, a damaged nonlinear spring was differentiated from a damaged linear spring. A testing protocol that shows potential for determining linearity and then conducting damage identification is presented. After this initial assessment is made, the analyst may choose whether to use the linear model of Chapter 3 to perform damage identification or to use a response surface model of the nonlinear system. It is shown that damaged nonlinear springs may be located with satisfactory accuracy, but the value of the stiffness coefficient cannot be estimated as accurately.

4.2 5DOF System With Noise

In order to see how the damage identification procedure defined in the previous chapter might work in an experimental environment, where variability is inevitable, noise was introduced in the natural frequencies.   Three percent normally distributed noise was added to each of the simulated, deterministic frequencies, $\omega_{nominal}$. This was calculated as

$$\omega_{noisy} = \omega_{nominal} * (1 + .03 * randn) \qquad (4.1)$$

where *randn* is the Matlab™ [20] function that generates random numbers drawn from a normal distribution with mean of zero and standard deviation of one. Five realizations of the full factorial set of 25 natural frequencies were used with the damage identification optimization algorithm, using the response surface model trained on the deterministic simulation (see Chapter 3).

Shown in Figure 4.1 are plots of the mean predicted values versus actual values for both stiffness coefficient and location. Normal confidence intervals (95%) were estimated on these means. In order to estimate the confidence intervals for a distribution of points, the following equations must be first solved for *d*, the standard normal value corresponding to 95% confidence, and then for *a*, the observation that is a part of distribution of interest and corresponds to the 95% confidence interval

$$\Phi(d) - \Phi(-d) = 0.95$$
$$-d < \frac{a - \mu}{\sigma} < d \qquad (4.2)$$

where Φ is the normal probability operator, and μ, the mean, and σ, the standard deviation, are both known. The value *d* may be obtained by using standard normal tables to do an inverse table lookup. The value *a* may then be found by solving the inequality. The same principle may be applied to finding confidence intervals on the mean, where instead of having an observation, *a*, an observation of the mean is used μ_a, and the variance is equal to $\sigma / \sqrt{n}$ where σ is the standard deviation of the distribution and *n* is the number of observations [24].
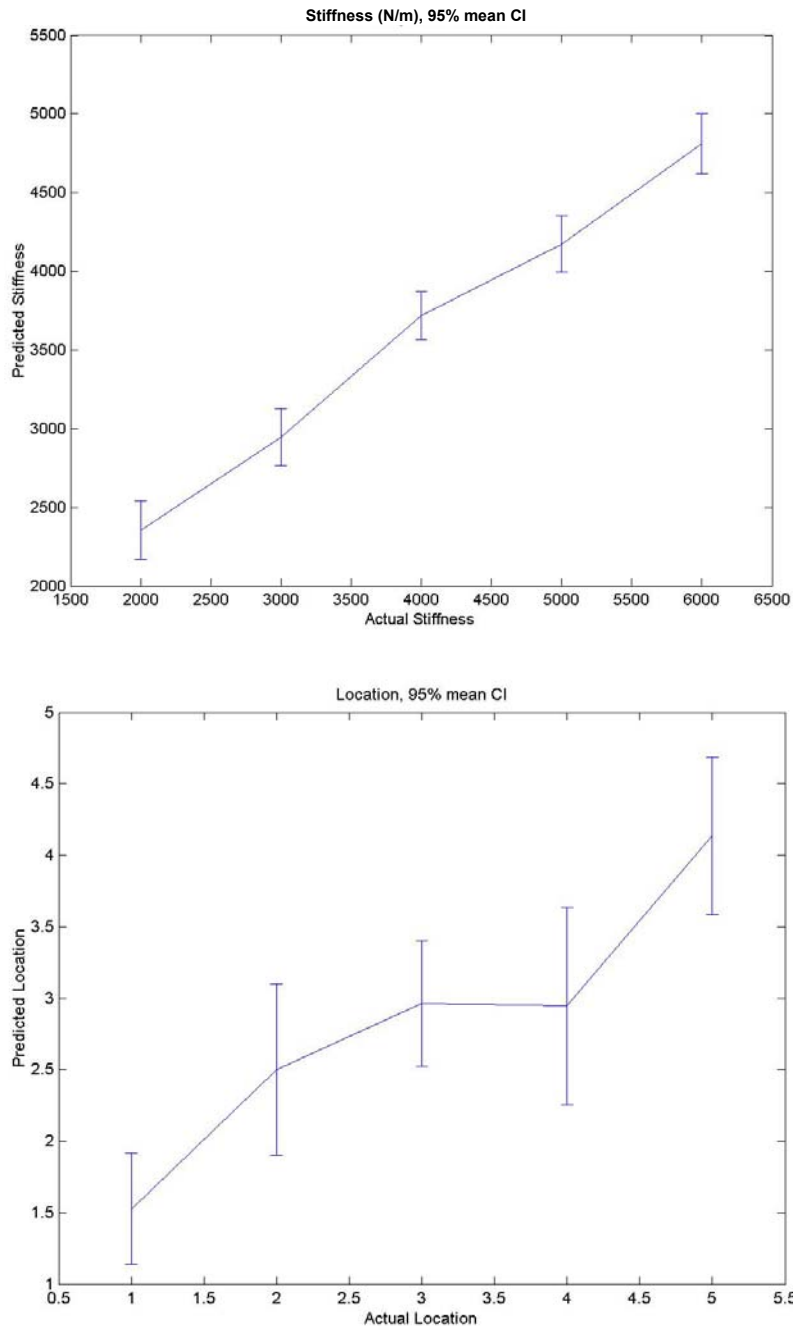
Figure 4.1 Upper and lower 95% confidence intervals on mean of 3% noise realizations.

Figure 4.1 demonstrates that the response surface model developed in Chapter 3 can positively identify changes in stiffness and some damage locations in the presence of simulated noise. The stiffness trend again errs conservatively below the actual values (shown as a straight line) at the higher levels. Because the confidence intervals overlap for Locations 2, 3, and 4, they are impossible to distinguish from each other, though they may be distinguished from Locations 1 and 5. This much is achieved by building a model based on 36% of the full factorial set of data, 9 of the 25 possible (more if continuous values of stiffness are used instead of five discrete values). Also recall that natural frequencies are derived using only data from Locations 3 and 5. From an efficiency standpoint, the method of damage identification using response surface metamodels yields a great deal of information even in the presence of simulated noise on the output features.

4.3 5DOF System with Nonlinearity

In reality, most structures exhibit nonlinearities, whether they are generated from Coulomb friction, material nonlinearities, excitation nonlinearities (such as a transient dynamics problem), *etc*. In order to demonstrate that response surface metamodels can be useful in identifying system nonlinearities, two models of a 5DOF system with a nonlinear spring were developed. In the first formulation, a discriminating parameter was incorporated so that a linear system could be differentiated from a nonlinear system. Damage was defined as either a linear reduced stiffness (less severe) or nonlinear spring replacing the linear spring (cubic nonlinear spring, severe damage) at a certain location. The second damage formulation involved defining damage as a nonlinear spring replacing a linear spring at a particular location (*i.e.*, damage is known to be nonlinear *a priori*). In this case, the damage was "less severe" because nonlinear spring constants were chosen so that displacements and forces were roughly in the same regime as linear.

For the screening model, the 5DOF system was identical to the linear 5DOF system of Chapter 3, with the exception of the linear stiffness term. In half of the cases a linear spring term was replaced by a nonlinear Kx^3 term (equivalent to a material hardening) for a variable location (1 through 5). The spring coefficient K (2000-6000 N/m or N/m^3) and location were the input parameters that were varied. Note that spring coefficients were numerically the same for both

the linear and nonlinear spring coefficients. This resulted in linear spring coefficients that were stiffer than the nonlinear cases.

Choice of output features was critical. Three features were chosen. They were maximum displacement (MD), spectral centroid (ST) and temporal centroid (TT). Recall that the temporal centroid, or normalized second moment of the displacement time history, is the time at which half of the energy has arrived and half is yet to come. The spectral moments (SM_1, SM_2, SM_3) are calculated in much the same way as temporal moments,

$$ SM_i = \int_{-\infty}^{\infty} \omega^i f(\omega)^2 \, d\omega $$

$$(4.3)$$

where SM_i is the spectral moment of interest, ω are the frequencies, i is the moment of interest (0, 1, 2, …) and f(ω) in this case is the magnitude of the transfer function [21]. The normalized second moment is the spectral centroid and a measure of which frequency bands possess the most energy. Because natural frequencies are often hard to discern when nonlinearities are introduced, the spectral centroid can be a good indicator of which frequency bands have the most power. A trade off must be accepted; in order to model nonlinear damage and discriminate between a linear and nonlinear system the features above were chosen instead of natural frequencies. Because natural frequencies are not the features of choice, the model's ability to capture linear damage may not be as good as that demonstrated in the previous chapter. However, it will be shown that if linear and nonlinear cases can be screened with high accuracy, then the analyst may revert to the model developed in Chapter 3 for the linear cases if necessary.

Next the design points had to be picked, by choosing a response surface design. The same face centered cubic design was chosen as that of Chapter 3. For this design, the mass was held constant at 7 kg, damping also was constant at 1 kg/s. The input parameters of stiffness coefficients (2000, 3000, 4000, 5000, 6000 $N/m^{1/3}$ or N/m) and locations (1-5) were used and a third parameter, "Linearity," was added. It was a categorical, or discrete parameter, meaning it could only be one of two values (as opposed to a continuum of values between a range). A value of 1 meant that the system was linear, implying that the stiffness coefficient was a linear spring

coefficient. A value of 2 meant that the system was nonlinear and the spring coefficient was nonlinear. Impulse magnitude was 5 N at Location 3 and response observations were made at Location 5.

An FCC design was again chosen, but this time it had 18 design points (the full factorial design was twice the size of the full factorial design in Chapter 3 because all points could be run at the linear and nonlinear settings, hence $2*5^2=50$ points). Nine runs were conducted for the linear system setup and the same nine runs were conducted for the nonlinear system setup. These points are shown in Table 4.1.

Table 4.1 FCC design used for damage identification of the nonlinear 5DOF system.

	Input Parameters			Output Features		
Design Point	Linearity (L or NL)	Stiffness (N/m or N/m$^{1/3}$)	Location	Maximum Displacement (m)	Temporal Centroid (TT, s)	Spectral Centroid (ST, Hz)
1	L	2000	1	0.03170	64.7387	6.3949
2	L	2000	5	0.03460	75.1915	8.2748
3	L	6000	1	0.03200	85.1324	8.4862
4	L	6000	5	0.03200	85.1324	8.4862
5	L	4000	1	0.03260	81.5699	7.7873
6	L	4000	5	0.03010	84.2039	8.4478
7	L	2000	3	0.04070	63.6015	7.1038
8	L	6000	3	0.03200	85.1324	8.4862
9	L	4000	3	0.03440	82.5572	8.0576
10	NL	2000	1	0.16830	52.6036	0.6983
11	NL	2000	5	0.00250	150.031	0.0101
12	NL	6000	1	0.13000	52.5364	0.9235
13	NL	6000	5	0.00520	51.4035	0.0606
14	NL	4000	1	0.14290	52.4482	0.8334
15	NL	4000	5	0.00410	94.9518	0.0228
16	NL	2000	3	0.19650	31.8629	1.0394
17	NL	6000	3	0.15260	31.8496	1.3799
18	NL	4000	3	0.16560	31.8484	1.2431

When the damage identification problem was solved for the full factorial set of points, the linearity parameter was identified with 100% accuracy. This screening result should not come as a surprise due to the fact that nonlinear damaged springs were "much softer" than the linear springs for the values of *knl* used, resulting in output features that were "very different" from the

corresponding output features of the linear cases. The results for stiffness and location predictions are shown below in Figures 4.2 and 4.3, and are sorted with respect to whether the predictions were for the linear case or the nonlinear case.

While the trend for both the linear and nonlinear stiffness coefficients is correct, both of their predicted distributions are very dispersed. For the linear case, the ranges for each value are wider then those predicted with the linear 5DOF model of Chapter 3, because the frequency features used in Chapter 3 are better suited to the linear system than the time series features of this study. The nonlinear ranges are also spread widely around the ideal line, although the trend is captured correctly (a good result considering the magnitude of damage imparted in the nonlinear cases). In both the linear and nonlinear springs, it would be difficult to distinguish what actual value an individual stiffness prediction might correspond to because of the way that the ranges of the predictions overlap.

Stiffness Predicted v. Actual
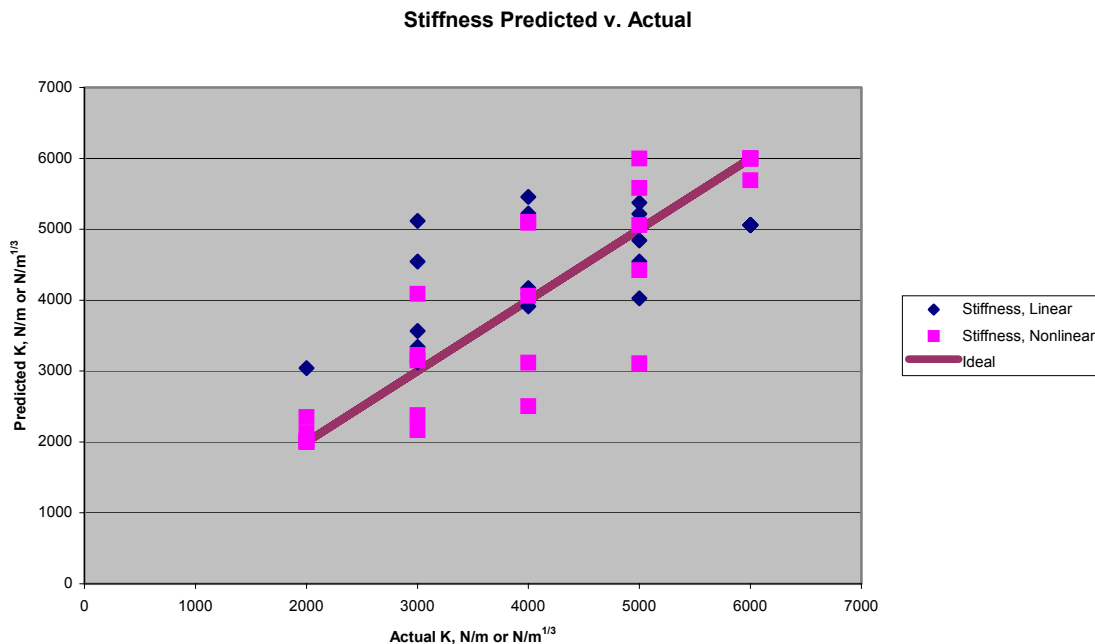
Figure 4.2 Stiffness predicted vs. actual.

Because the model is able to screen for linearity with 100% accuracy, an appropriate metamodel might be chosen on this basis. For example, if the identification predicts that the system is linear, then employment of the response surface model developed in Chapter 3 is suggested,

because it provided more accurate predictions of linear stiffness coefficients (because the output features of natural frequency were better suited to a linear system). If the model predicts that the system is nonlinear, inaccuracies in stiffness predictions of the current model are unavoidable at this stage.

In contrast to the poor stiffness predictions of the nonlinear system, in Figure 4.3, it can be seen that locations for the nonlinear model are predicted very well. Predictions lay in tight clusters near the 45° line that indicates what "ideal" predictions should be. It should be noted that Locations 4 and 5 could be indistinguishable because of the overlap in the range of their predicted values. It can also be seen in Figure 4.3 that linear location predictions are not good. However, the screening procedure suggested above should be applied for prediction of location as well. If the system is shown to be linear, use of the response surface model of Chapter 3 is suggested for greater accuracy.

Location Predicted v. Actual
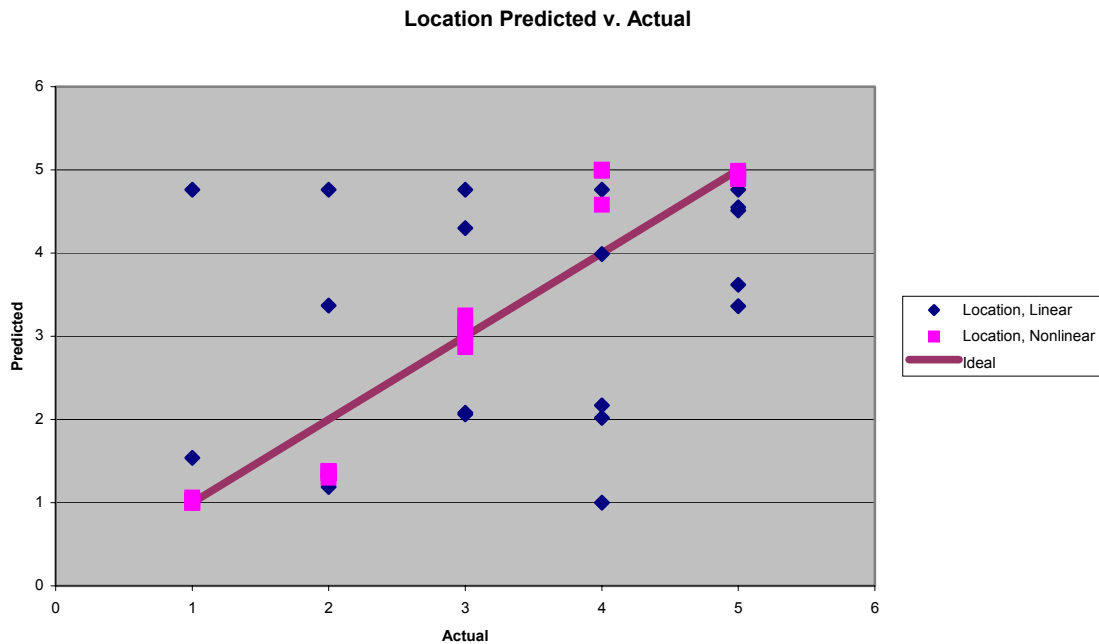
Figure 4.3 Location predicted vs. actual.

In the second kind of damage configuration, it is assumed that damage is known to be nonlinear. A nonlinear spring (in the form of a kx^3 term replacing the linear spring) was introduced as

"damage" at one of the 5 locations. The nonlinear spring with varying stiffness coefficient was chosen such that it resulted in static displacements that were in the same regime as the linear case. "Healthy" was again defined as all linear springs with stiffness coefficient set at 6000 N/m. Damage was defined as a nonlinear spring replacing a linear spring at any of the five locations. Degree of damage was defined as the value of the nonlinear spring coefficient: 6e6, 7e6, 8e6, 9e6, 1e7 N/m$^{1/3}$.

Again, a 9 run fraction of the full factorial design space (25 runs) was used to formulate relationships between controllable inputs and measurable outputs. Because of the presence of nonlinearities in the system, natural frequencies were not chosen as output features because they were more difficult to identify. Instead maximum displacement and spectral and temporal moments were chosen.

Results from the damage identification procedure are shown in Figure 4.4. Optimizations for the design set and the full factorial set have been plotted separately for both location and nonlinear stiffness coefficient (knl). Location is predicted well (with one exception) for both the design set and the additional points of the full factorial set. Nonlinear stiffness is predicted reasonably well for the design set (errors of less than 15%). However stiffness predictions for those points outside of the training set are significantly worse (errors over 20% in a few cases).

For the case of the nonlinear 5DOF system, in which damage is a nonlinear spring with varying stiffness coefficient inserted at one of the five possible locations, response surface metamodels again show promise in their ability to predict degree and location of damage in this simple, simulated system. In this example, location was predicted satisfactorily for all 25 simulated sets (with one outlier) and the stiffness coefficient was predicted well for the design set. Again, this much was accomplished with training on only nine of the 25 possible sets. The use of displacement, temporal and spectral moments as output features was explored and warrants further investigation for use in nonlinear damage identification problems. Use of additional training sets and/or features may be necessary to improve the stiffness predictions.
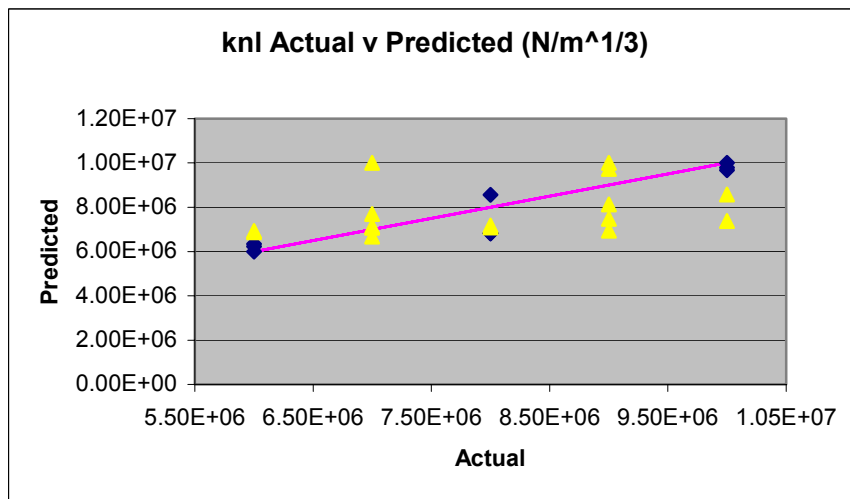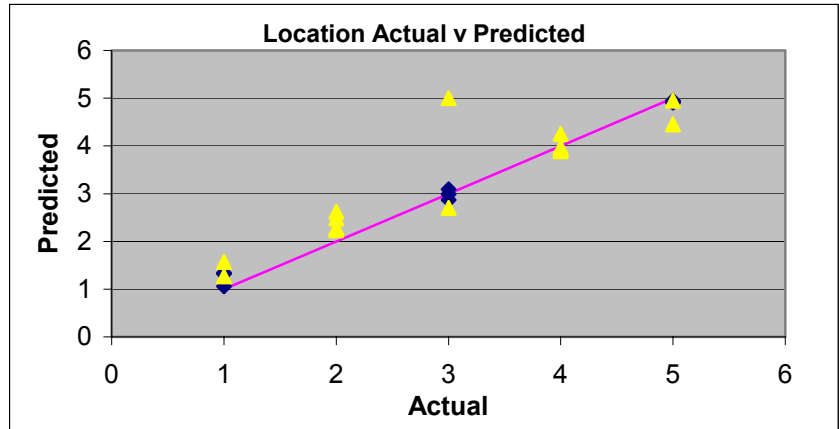
Figure 4.4 Results from damage identification using response surface metamodels developed for a nonlinear system (Blue Diamonds are points belonging to the design set, yellow triangles are points outside of the design set, the line is where the values should ideally plot).

4.4 Conclusions

Response surface metamodels show potential to be robust to noise and nonlinearities with some limitations. With 3% noise introduced on the natural frequency features of the linear 5DOF model, predictions of the changed stiffness and its location were still satisfactory given the limited amount of data used for generation of the response surface metamodels. For the case of a severely damaged nonlinear spring, the response surface metamodels were able to successfully locate a the damage, but were not able to quantify the stiffness coefficient of that spring using the features chosen. RSMs were also used to differentiate between a linear and nonlinear data set for given impulse magnitude and location, and response observation location, with 100% accuracy

in these predictions. When simulating lower levels of damage with the nonlinear springs, it was shown that response surface metamodels could predict damage location well for all points tested and could predict stiffness well for the design set. A protocol for screening and then choosing an appropriate RSM for damage identification was demonstrated for the system studied and shows potential for use in other systems.
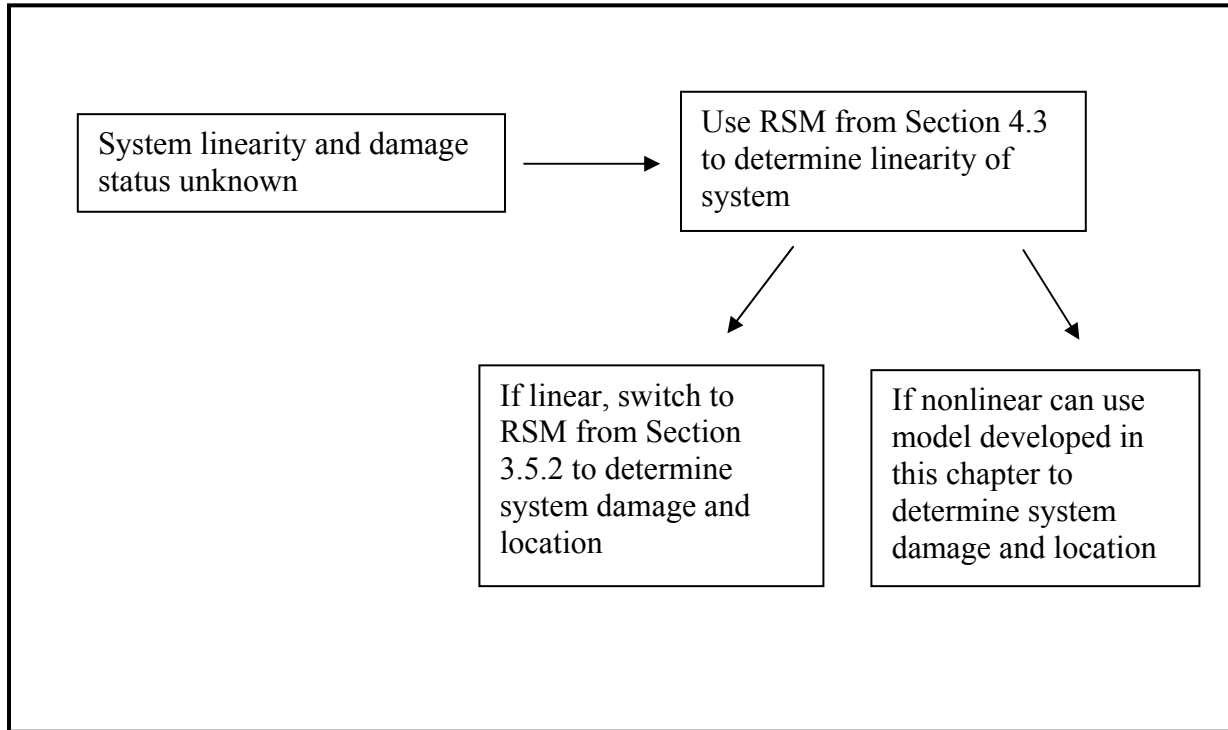
Figure 4.5 Flowchart of protocol for use in choice of response surface models.

Chapter 5

BEAM DAMAGE IDENTIFICATION PROBLEM

5.1 Introduction

This chapter will demonstrate how the methodologies of Chapters 3 and 4 may be applied to a more realistic problem. In real applications it is anticipated that response surface metamodels will be used in the experiment-simulation environment. For example, engineers may be interested in identification of damage on an *in situ* component, such as a bridge girder or an aircraft wing. In this sort of situation, simulation must be used to train metamodels, because it would be impractical or even impossible to actually damage structures. In the spirit of this sort of philosophy, a simple simulation and experiment were constructed, and response surface metamodels built to do damage identification. The protocol suggested by the flowchart of Chapter 4, section 4.3 suggests initial determination of system linearity. The system studied in this chapter is, by design, linear and hence the protocol further suggests applying the steps outlined in Chapter 3. These are the steps presented in the following sections.

5.2 Step1: System Description

The system is a beam with ten potential locations at which small masses may or may not be attached. The beam is aluminum with a stiffness of E=70.3 GPa and density 27.5 kN/m^3. Dimensions are as shown in Figure 5.1. The masses are secured to both sides of the beam with wax at a particular location. The mean of the masses is 1.34 g (they are nominally the same).

Figure 5.2 is a photo of the experimental setup, showing masses in place. The beam is excited using a piezo-ceramic patch (PZT) and sensing is also done using a PZT. Both PZTs are located

near the fixed end of the beam. The excitation signal was random with a 1 kHz bandwidth. This allowed the first ten natural frequencies to be found.
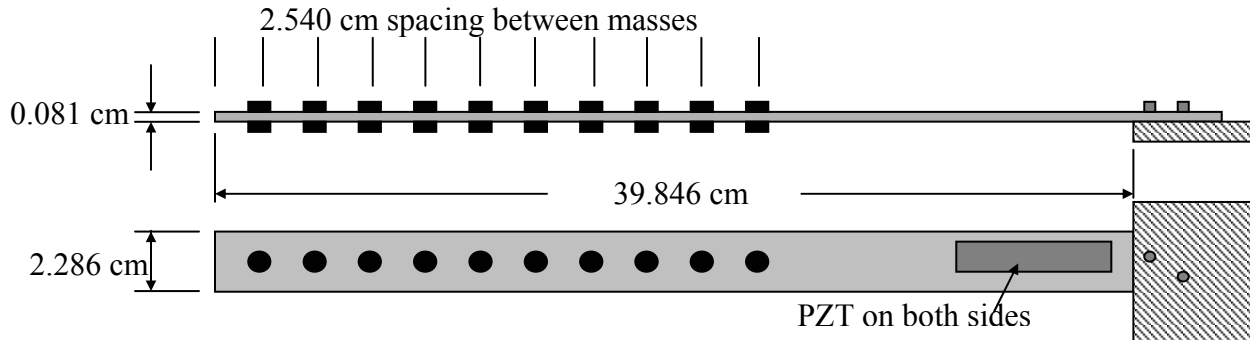
Figure 5.1 Beam dimensions and mass spacing. Direction of vibration is out of the page.

Figure 5.2 Photo of the experimental beam-mass setup.

An Ansys™ model of this experiment was designed [25], shown in Figure 5.3. The model used 14 2D beam elements. The masses were represented as point masses at the location of the center of the actual mass. PZT mass and stiffness were neglected. Boundary conditions imposed at the end of the beam were zero rotation and displacement. Modal analysis was performed using a Lanczos solver. In order to "validate" the finite element model, the first ten natural frequencies with all the masses on and the first ten natural frequencies with all the masses off were compared to the corresponding experimental results. Only two setups were used for comparison, because to be true to the spirit in which metamodels will actually be used, it is assumed that experimental

budgets will be limited in real world situations. Results of the test-analysis correlation are shown in Tables 5.1 and 5.2 (the Relative Error metric is further explained in Appendix A).
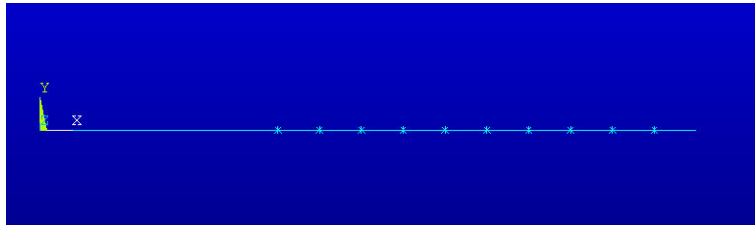
Fig 5.3 Ansys™ 2D beam simulation with point masses.

Table 5.1 Test-analysis correlation for experimental setup and finite element model: all masses removed (Mode 10 not shown because frequency was higher than 1000 Hz).

Mode number	Experimental Frequency (Hz)	Simulation Frequency (Hz)	Relative Error (%)
1	3.7500	3.9700	5.8
2	24.070	24.870	3.4
3	67.190	69.640	3.7
4	130.31	136.47	4.7
5	217.81	225.59	3.4
6	325.94	336.99	3.4
7	456.25	470.67	3.2
8	607.19	626.62	3.2
9	784.06	804.85	2.7

Table 5.2 Test-analysis correlation for experimental setup and finite element model: all masses present.

Mode number	Experimental Frequency (Hz)	Simulation Frequency (Hz)	Relative Error (%)
1	3.7500	2.3300	37
2	16.880	15.260	9.6
3	46.560	47.080	1.1
4	96.880	97.740	0.9
5	156.56	159.03	1.6
6	229.06	230.73	0.7
7	331.56	328.45	0.9
8	443.13	443.40	.06
9	551.25	552.97	0.3
10	696.56	679.97	2.3

For the most part, it can be seen that differences in the natural frequencies are less than 5%. A few explanations are posed for the high error on Modes 1 and 2 with masses on the beam. Experimental values were derived using the highest resolution possible in a 1000 Hz window (separation of points is 0.313 Hz). For low frequencies, this may not be enough resolution. That is, an error of +/- 0.313 Hz out of 3 Hz is about 10% already. In addition to the resolution problem, placement of masses is likely to affect the first two modes more than higher modes. Placement of masses was only as accurate as "by eye" can be. Another possible source of this disagreement may be neglecting the PZT mass and stiffness in the simulation. Despite these outliers, it was decided that the FEM was an adequate representation of the laboratory experiment based on the good agreement of the other modes.

5.3 Step 2: Definition of Input Parameters and Output Features

Model input parameters were undamaged, "mass on" (1), or damaged, "mass off" (0), at each of the ten locations (L1-L10, where L1 is near the cantilevered end, and L10 near the fixed end). Input parameters were categorical, or discrete, meaning they could only have a value of 1 or 0. Because the beam was assumed to be linear, the first ten mode frequencies were chosen for output features. Because of the fundamental physical relationship between mass and system frequency, variable screening was deemed unnecessary.

5.4 Step 3: Construction of Response Surface Model and Error
   Characterization

The full factorial design for the beam-mass setup would consist of (2 input parameters levels)$^{(10 \text{ input parameters})}$ = 1024 simulation runs or experiments. A 1/32 factorial design was chosen with 32 design points. In this case simulation runs were used to generate the output features corresponding to the input parameter setups. The full set of design points is shown in Appendix C. Recall that each output feature has its own model associated with it. Adjusted R^2 values (See Appendix A for calculation of this error metric) are given in Table 5.3 for each model. It can be seen that all the Adjusted R^2 values are very close to 1, indicating that the models are good fits to the 32 design points.

5.5 Step 4: Damage Identification

Once the response surface models were constructed, they were then used for damage identification. In this case, damage is defined as "mass removed." To start with, the design points were run using the inverse problem formulation – that is, assuming the set of 32 design point frequencies has been simulated and are known, how many masses were present and at what locations were they on the beam? In this first set of simulations we seek to characterize the error of the inverse problem formulation due to error between simulation and metamodel for the 32 design points.

Table 5.3 Adjusted R^2 for each model generated using the set of 32 design points.

Model of Output Feature	Adjusted R^2
ω_1	0.9801
ω_2	0.9481
ω_3	0.9294
ω_4	0.8851
ω_5	0.8918
ω_6	0.9216
ω_7	0.9809
ω_8	0.9536
ω_9	0.8130
ω_{10}	0.8993

Because all factors were discrete, the optimizer used to work the inverse problem performs somewhat differently.   Instead of a Nelder-Meade simplex optimization routine that was implemented before, the optimizer embedded in the Design Expert software simply tries all possible combinations of points (in this case 1024 points) and ranks them using the desirability function described in Chapter 3, Section 3.5.2. Computation of all 1024 points is not intensive, because only the metamodels are evaluated. Again, desirability values close to one are best, indicating that the output features (mode frequencies) are very near the target values specified by the user. The set of input parameters associated with the highest value of desirability was chosen as the predicted set of masses and locations associated with the specified frequencies.

The results of optimization on the 32 design points is shown below in Figure 5.4 and 5.5. All ten frequency models were used. First, just the number of masses predicted is examined in Figure 5.4. It can be seen in the figure that the predictions are most accurate when the actual number of masses is five or six, which makes sense because there were far more training points with five or six masses. At extreme values, such as two masses on the beam or all ten masses on the beam, the models tend to over and under estimate, respectively. However it is clear to see that the inverse formulation captures the main trend for the predicted number of masses on the beam which is expected, because the simulated design point frequencies were used.
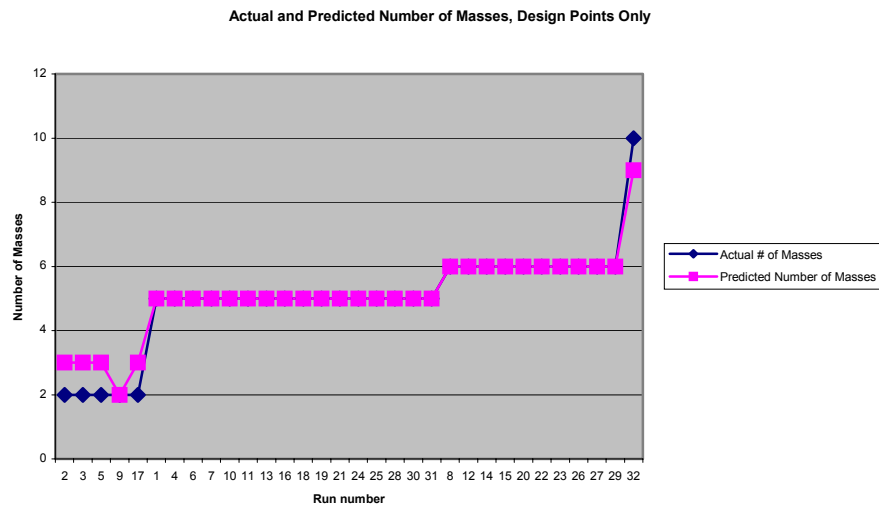
Figure 5.4 Predicted and actual number of masses for the set of design points.

Next we examine how well the masses were located in Figure 5.5. For each location, the number of correct identifications of mass, the number of false positives (mass predicted when none actually there), and the number of false negatives (mass not predicted when mass actually there) are shown in Figure 5.5. Locations near the free end of the beam are predicted better than locations near the fixed end. However error for all locations over the set of design points is small, possibly because the resonant frequencies are more sensitive to mass loading at the tip of the beam than near the cantilevered end. The next question to answer is, "Do points that are not in the design set follow the error trends exhibited by the design set?"

Because the full factorial set of points consists of 1024 points, it is not feasible to run every possible combination of masses on the beam, either simulated or experimentally. In order to get an idea of how at least some points outside of the design set might be predicted by the response
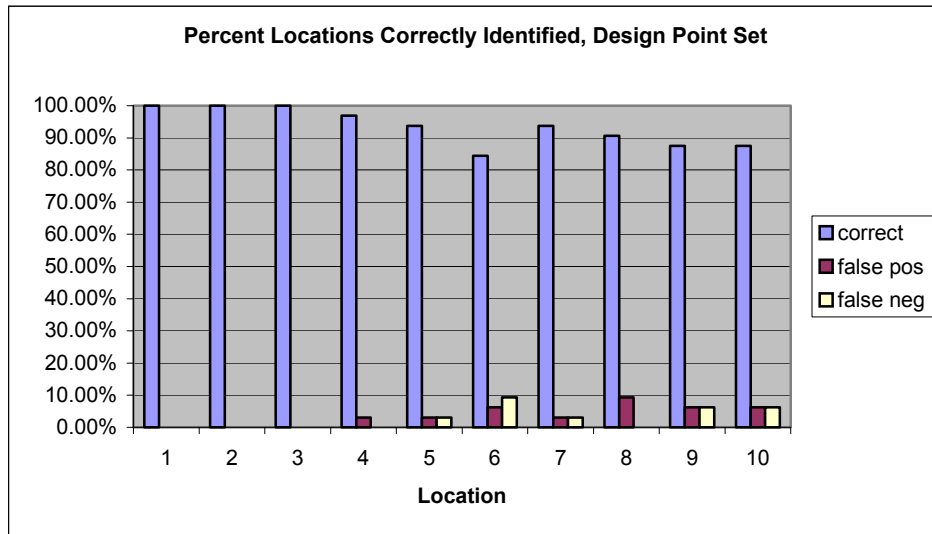
Figure 5.5 Percent of design points identified correctly.

surface model, subsets of points were chosen to characterize error in the damage identification problem. Ten points were chosen to characterize the error of points outside the design set using the response surface models developed. Simulated frequencies were used to predict number of masses and locations. In this case, error in the inverse formulation due to error between the simulation and metamodel for points outside of the design set was characterized. The actual mass locations are shown in Table 5.4, three runs with 7 masses, three runs with 8 masses, and 4 runs with 9 masses were created. More mass was chosen because there were fewer design points at these settings and because characterizing "less damaged" states may be more helpful to the analyst. It is anticipated that response surface metamodels will be most helpful when structures are not in their most severely damaged states.

Figure 5.6 again shows error in the prediction of the number of masses on the beam. If there is error in the predictions, it is because fewer masses were predicted than were actually there (conservative). This trend is in agreement with the trend seen in the set of design points for more

mass on the beam. It can be seen in Figure 5.7 that the error in the predictions of location is also somewhat similar to the error seen on the design set. Locations near the free and fixed end of the beam have more correct predictions then those locations in the middle of the beam.

Table 5.4 Actual mass locations for points generated for simulated natural frequencies outside of the design set .

Error Run	L1	L2	L3	L4	L5	L6	L7	L8	L9	L10
1	1	1	1	1	1	1	1	0	0	0
2	1	1	1	1	0	0	0	1	1	1
3	1	0	1	1	0	1	1	0	1	1
4	0	0	1	1	1	1	1	1	1	1
5	1	1	0	1	1	1	1	0	1	1
6	0	1	1	1	1	1	1	1	1	0
7	1	1	1	0	1	1	1	1	1	1
8	1	0	1	1	1	1	1	1	1	1
9	1	1	1	1	1	1	1	1	1	0
10	1	1	1	1	1	1	0	1	1	1
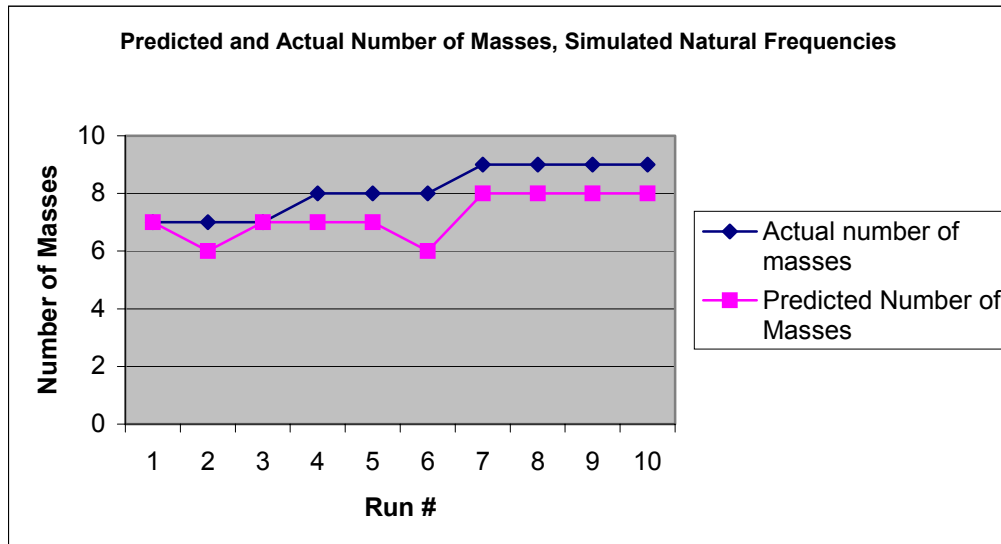
Figure 5.6 Actual and predicted number of masses for simulated natural frequencies outside of the design set.

Percent Correct Locations, Simulated Natural Frequencies
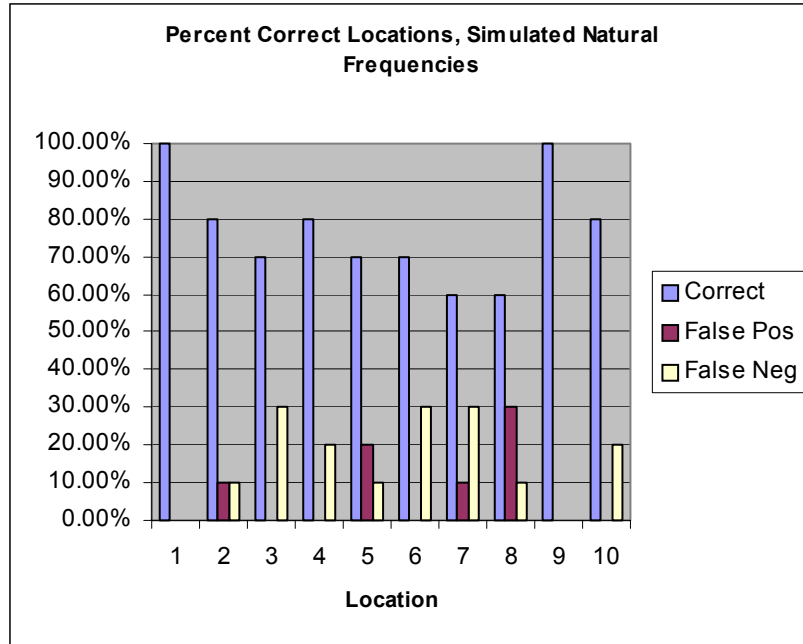
Figure 5.7 Location error for simulated natural frequencies outside of the design set.

The final set of points was generated to examine how use of experimental natural frequencies in the RSMs designed with ANSYS™ simulated frequencies would affect predictions of mass and location. For this set of points (shown in Table 5.5 below), the natural frequencies were generated using the experimental setup described in Section 5.2. This set of points may be thought of as a measure of how robust the inverse damage identification process is to frequencies generated in an experimental environment. Seven of these points corresponded to design points, so a one-to-one comparison could be made between simulation frequencies and experimentally measured frequencies. The remaining five points again concentrated on the cases of "more" mass on the beam. These frequencies were used to perform damage identification and results are shown in Figures 5.8 and 5.9. Frequency 1 was not used in damage identification, because it was the same value for all experimental runs (3.75 Hz), which was probably due to the resolution of the window (0.313 Hz) being too large to capture changes in the first frequency. Frequency 10 was not used for Run 7 with all masses removed because the tenth frequency was outside of the experimental 1000 Hz window.

Table 5.5 Mass locations for experimentally generated natural frequencies.

Run	Description	L1	L2	L3	L4	L5	L6	L7	L8	L9	L10
1	DP1	0	0	0	0	0	1	1	1	1	1
2	DP 6	1	0	1	0	0	1	1	0	1	0
3	DP 12	1	1	0	1	0	0	1	0	1	1
4	DP 18	1	0	0	0	1	0	1	1	1	0
5	DP 24	1	1	1	0	1	0	1	0	0	0
6	DP32/ validation run	1	1	1	1	1	1	1	1	1	1
7	0 masses/ validation run	0	0	0	0	0	0	0	0	0	0
8	9 masses	1	1	1	0	1	1	1	1	1	1
9	8 masses	0	1	1	1	0	1	1	1	1	1
10	7 masses	1	1	1	1	1	1	0	1	0	0
11	8 masses	1	1	0	1	1	1	1	1	1	0
12	7 masses	0	0	1	1	1	1	0	1	1	1

Table 5.6 is the error between simulation and experiment frequencies for the 7 runs that were in both the design set and the experiment-RSM error characterization set. With the exception of Frequency 2, nearly all of the frequencies are over estimated by the simulation (although not by much). Knowing that the response surface model we are using has been trained on the simulation data (frequencies higher than experiment), we would expect the response surface model to tend to under estimate the number of masses on the beam (fewer masses would result in higher frequencies). When the optimizer is used with the experimental frequencies (lower than those that the model was trained on), the model will be "fooled" into thinking that there are fewer masses on the beam than actually are present. Figure 5.8 shows that this is not a bad assumption to make. With two exceptions, if there is error in the predicted number of masses, it is lower than actual number of masses. This error again follows the general trend of the design set.

Table 5.6 Percent error between experimental frequencies and simulated frequencies.

Run	ω_2	ω_3	ω_4	ω_5	ω_6	ω_7	ω_8	ω_9	ω_{10}
1	-4.69%	0.13%	3.43%	2.66%	1.07%	1.55%	1.53%	0.21%	1.12%
2	-5.68%	2.36%	3.78%	2.24%	2.91%	2.23%	2.94%	3.10%	-1.66%
3	-8.69%	1.43%	3.09%	4.95%	0.96%	0.33%	2.74%	0.72%	3.53%
4	-9.65%	1.79%	4.71%	2.62%	1.00%	1.68%	2.28%	0.68%	0.40%
5	-6.59%	2.94%	2.04%	0.70%	-0.30%	2.31%	-0.29%	2.62%	3.80%
6	-9.56%	1.11%	0.90%	1.58%	0.73%	-0.94%	0.06%	0.31%	-2.38%
7	3.36%	3.65%	4.73%	3.57%	3.39%	3.16%	3.20%	2.65%	N/A
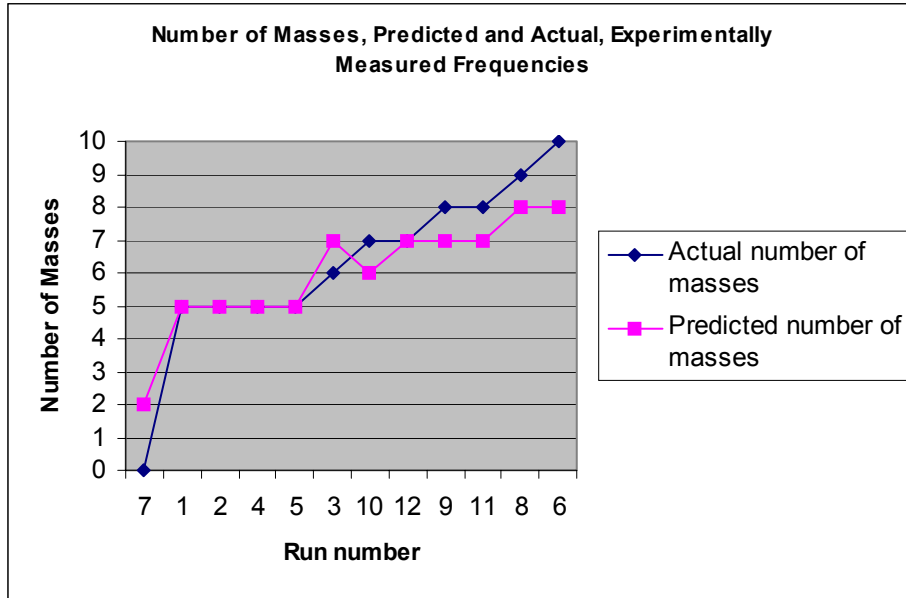
Figure 5.8 Actual and predicted number of masses using experimentally measured frequencies

In Figure 5.9 we can see that with the exceptions of locations 1 and 2, near the free end of the beam, all other location predictions are correct over 70% of the time. This much is accomplished using response surface models trained on a simulated set of frequencies (that was only $1/32^{nd}$ of the full factorial set of points) with experimentally generated frequencies.
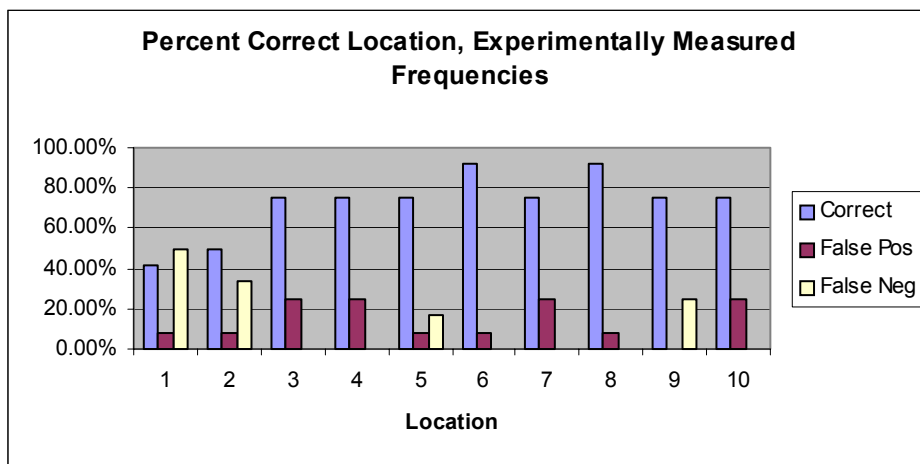
Figure 5.9 Location error when experimentally measured frequencies are used.

In summary, for the design set the number of masses is predicted well (within one or two of the actual number), tending to err conservatively at less "damaged" levels. Both of the error characterization sets confirm this trend. For the two sets tested with simulated frequencies, location is predicted correctly about 85% of the time. For the set tested with experimental frequencies, location is predicted about 70% of the time.

5.6 Conclusions

This chapter has shown how the four-step process of Chapter 3 may be applied to a more realistic problem that involves both simulated and experimental data. The response surface models developed for the beam-mass system using natural frequencies again as output features are quite successful at predicting the number of masses on the beam and do a reasonable job locating masses given the limited amount of data they were trained with. Two error sets were examined, one which used simulated frequencies outside of the design set and one that used experimentally measured frequencies. Results for all sets were encouraging, with correct trends captured for number of masses on the beam and locations predicted correctly, often more than 70% of the time. The response surface based damage identification method does well given the uncertainties inherent in the simulation-experiment environment and the $1/32^{nd}$ factorial training set. It has also been shown that the uncertainty present may be quantified to some extent.

Chapter 6

CONCLUSIONS AND FUTURE WORK

6.1 Introduction

This thesis has shown that response surface metamodels may be used in structural damage identification problems. A four-step methodology has been developed and was demonstrated on two dynamic structural systems. The models developed in this thesis have been shown to be robust to experimental noise and have shown promise for use in nonlinear systems. Response surface metamodels have also proven useful in the context of reduced order modeling, providing much information about a system given a limited amount of data.

6.2 Key Results

A four-step process was defined for doing damage identification with response surface metamodels. This process was first demonstrated on the linear 5DOF system and then applied to the beam-mass system. Definition of input parameters and output features plays a key role in how effectively response surface metamodels may be applied to damage identification problems. Input parameters must be "damage indicators." In this case mass and stiffness were used along with the location of the damage. It is important that output features used provide independent information about the system. For a linear model, like the linear 5DOF system or the beam-mass system, natural frequencies work well. For nonlinear models, time series features such as maximum displacement or the centroid of the displacement time history energy, as well as single number representations of the frequency domain data (centroid of the energy of FRF) performed reasonably well.

Damage identification was performed on the 5DOF system with acceptable accuracy using only nine design points and measurements taken at only two of the five locations. Similarly identification of number of masses and their location on a beam was performed using only a small fraction of the total possible points (1/32nd of the full factorial design set) using both simulated and experimental data.

Robustness of RSMs to variability on the output features has been demonstrated. The linear 5DOF system had 3% normally distributed noise introduced on its natural frequency output features. The model was still able to locate and predict the magnitude of a damaged spring in the system with some limitations. RSMs were also used to locate and quantify number of masses on a beam when experimentally measured frequencies were used instead of the simulated, deterministic frequencies that the RSMs were trained on.

Finally, the ability of response surface metamodels to locate and predict the spring coefficient of a nonlinear spring replacing a linear spring in the 5DOF system was assessed. Features better suited to a nonlinear system setup than natural frequencies were used. They were maximum displacement, centroid of the energy of the displacement time history and centroid of the energy of the FRF. Using these features and a limited amount of training data, location was predicted quite well but spring coefficient was not as accurate. This model was also able to discriminate between a linear system and a nonlinear system with 100% accuracy, suggesting that a screening procedure be employed if system linearity is not known. Once linearity is assessed, the appropriate model may be chosen.

6.3 Contributions

In this thesis, it has been shown that response surface metamodels show potential for use in damage identification scenarios. RSMs were developed for simple physical systems and damage identification was performed successfully, given the limited amount of "training" data used. Error of the RSMs was characterized. They were shown to be robust to noise and were applied in an experiment/simulation environment successfully. The RSM in its inverse formulation was also used successfully to determine system linearity for the 5DOF example presented in this thesis. To date, there are no known studies that demonstrate the potential of response surface

metamodels, in their inverse formulation, on simplified damage identification problems. To fill this void, the potential of RSMs has been demonstrated in this thesis. It is recommended that these models be further developed and their use in structural health monitoring and damage prognosis problems be considered.

6.4 Recommendations for Future Work

The models developed in this thesis suggest that response surface metamodels are reduced order models that could be employed for damage identification of dynamic structures. However, only very simple systems have been used for demonstration of the use of RSMs to do damage identification. A wider range of dynamic systems should be examined. Damage indicators in this thesis have focused on changing stiffness and mass parameters. Future models should incorporate changes in damping as a damage indicator, as it has also been proven as a damage indicator ([26], for example). Response surface designs could also be coupled with neural networks. Training points could be chosen using design of experiments methods and the mapping between input parameters and output features could then be established by the neural networks. Response surface metamodels should also be considered for application in the realm of structural health monitoring and damage prognosis, where their small computational requirements could be helpful for on-board damage identification.

References

[1] Tanner, N. A., Farrar, C. R., and Sohn, H., 2002, "Structural Health Monitoring Using Wireless Sensing Systems with Embedded Processing." *Journal of Intelligent Materials Systems and Structures*, Submitted for publication.

[2] Robertson, A. N., Sohn, H., Bement, M. T., Hunter, N. F., Liu, C., and Farrar, C. R., 2003, "Damage Diagnosis and Prognosis for Composite Plates," accepted to 21st International Modal Analysis Conference, Kissimmee, FL.

[3] Myers, R. H., and Montgomery, D. C., 1995, *Response Surface Methodology*, John Wiley and Sons, Inc., New York, NY.

[4] Butler, T. A., Hemez, F. M., Schultze, J. F., Sohn, H. , Doebling, S.W., 2001, "Model Validation for a Complex Jointed Structure," 19th International Modal Analysis Conference, Kissimmee, FL.

[5] Masson, G., and Hemez, F. M., 2002, "Model Reduction Primer," Los Alamos National Laboratory internal publication, Los Alamos, NM.

[6] Masson, G., Cogan, S., Bouhaddi, N., Lombard, J. P. and Bonini, J., 2002, "Parameterized Reduced Models for Efficient Optimization of Structural Dynamic Behavior," AIAA-2002-1392, American Institue of Aeronautics an Astronautics.

[7] Bobillot, A. and Balmés, E. 2002, "Iterative Techniques for Eigenvalue Solutions of Damped Structures Coupled with Fluids," AIAA-2002-1391, American Institute of Aeronautics and Astronautics.

[8]   Burton, T. D., Hemez, F. M., and Rhee, W., 1999, "A Combined Model Reduction/SVD Approach to Nonlinear Model Updating," 17th International Modal Analysis Conference, San Antonio, TX.

[9]   Doebling, S. W., Farrar, C. R., and Prime, M., 1998, "A Review of Damage Identification Methods that Examine Changes in Dynamic Properties," *Shock and Vibration Digest*, 30(2).

[10] Brockman, A., Clough, J., Mulji, K., and Hunter, N.F., 2001, "Identifying the Effects of Stiffness Changes in a 5-DOF System," 19th International Modal Analysis Conference, Kissimmee, FL.

[11] Lee, U., Kim, N. and Shin, J., 2001, "Identification of Damages within a Plate Structure," A01-25047, American Institute of Aeronautics and Astronautics.

[12] Rutherford, B., 2002, "Response-Modeling for the Design of Computer Experiments," 20th International Modal Analysis Conference, Los Angeles, CA.

[13] Stat-Ease, 2000, *Design Expert 6.0.5* User's Manual and Software, Minneapolis, MN.

[14] Huh, J. and Haldar, A., 2001, "Stochastic Finite-Element-Based Seismic Risk of Nonlinear Structures," *Journal of Structural Engineering*.

[15] Gao, X., Low, T.-S., Chen, S., and Liu, Z., 2001, "Structural Robust Design for Torque Optimization of BLDC Spindle Motor Using Response Surface Methodolgy," *IEEE Transactions on Magnetics*, 37(4).

[16] Meckesheimer, M., Barton, R. R., Simpson, T., Limayem, F., and Yannou, B., 2001, "Metamodeling of Combined Discrete/Continuous Responses," AIAA Jounral, 39(10).

[17] Hemez, F. M., Wilson, A. C., and Doebling, S. W., 2001, "Design of Computer Experiments for Improving an Impact Test Simulation," 19th International Modal Analysis Conference, Kissimmee, FL.

[18] Cundy, A. L., Schultze, J. F., Hemez, F. M., Doebling, S. W., and Bingham, D., 2002, "Variable Screening Methods in Metamodel Design for a Large Structural Dynamics Simulation," 20th International Modal Analysis Conference, Los Angeles, CA.

[19] Shinn, R., Hemez, F. M., and Doebling, S. W., 2003, "Estimating the Error in Simulation Prediction Over the Design Space," 44th AIAA/ASME/ASCE/AHS Structures, Structural Dynamics, and Materials Conference, Norfolk, VA.

[20] The Mathworks, 2001, *Matlab 6.1*, Software and Toolboxes, Natick, MA.

[21] Smallwood, D. O., 1994, "Characterization and Simulation of Transient Vibrations Using Band Limited Moments," *Shock and Vibration*, 1(6).

[22] Hemez, F. M. and Doebling, S. W., 2003, "From Shock Response Spectrum to Temporal Moments and Vice-Versa," accepted to 21st International Modal Analysis Conference, Kissimmee, FL.

[23] Inman, D. J., 2000, *Engineering Vibration, 2nd Ed.*, Prentice Hall, Upper Saddle River, NJ.

[24] Ang, A. H.-S., and Tang, W. H., 1975, *Probabilty Concepts in Engineering Planning and Design*, John Wiley and Sons, New York, NY.

[25] Ansys, Inc., 1994, *Ansys 6.0* Software.

[26] Banks, H. T., Inman, D. J., Leo, D. J., and Wang, Y., 1996, "An Experimentally Validated Damage Detection Theory in Smart Structures," *Journal of Sound and Vibration*, 191(5).

Appendix A

ERROR METRICS: HOW TO DECIDE WHICH RESPONSE SURFACE FITS BEST

Any model of a simulation or experiment is subject to inaccuracies. Error could be caused by, among other things, numerical error in simulation code, environmental variability in experimental testing, calibration errors, or inability of the model to capture all of the underlying physics of the problem. The most useful model will be the one that best captures the output feature of interest over the broadest area of the response space. In order to compare models, error metrics must be defined.

R^2, a measure commonly used in regression analysis, is a statistic that estimates Pearson's correlation ratio. It is a measure of the reduction in variability in the output feature through the use of the input variables chosen for the model [3]. In equation form

$$R^2 = 1 - \frac{\sum error^2}{\sum Out^2} \qquad (A1)$$

where *error* is the difference between actual output feature values and predicted values and *Out* is the actual output feature values. R^2 may be adjusted for the number of terms (or coefficients) in the polynomial model and may be estimated for prediction as well. These values can serve as one method of comparing models; values near 1.00 indicate good fit, values near 0.00 indicate poor fit. However regression analysts warn not to use R^2 as a definitive measure of how good a model is. Meyers and Montgomery [3] note "a large value of R^2 does not necessarily imply that

the regression model is a good one. Adding a variable to the model will always increase R^2, regardless of whether the additional variable is statistically significant or not." Adjusted R^2, on the other hand, does not always increase as terms are added to the model. It can be expressed as

$$R^2_{adj} = 1 - \frac{(n-1)}{(n-p)}(1-R^2) \qquad\qquad (A2)$$

where n is the number of observations of the output feature and p is one plus the number of terms in the model [3].

Another metric of comparison can be as simple as calculation of mean square error

$$MSE = 100 * \frac{\sum(Actual - Pred)^2}{n*(\sigma_{Actual})^2} \qquad\qquad (A3)$$

where n is the number of experiments conducted, *Actual* and *Pred* are the actual and predicted values of the output feature, and σ_{actual} is the standard deviation of the actual values of the output feature. Relative error might also be used

$$RE = 100 * \frac{\sum(Actual - Pred)^2}{\sum Actual^2} \qquad\qquad (A4)$$

The first set of models designed for the 5 DOF simulation had only two factors, impulse magnitude and stiffness. Each of these parameters was varied over three to five levels depending on the design used. Resulting error metrics are summarized in Table A1 below (Taguchi and D-Optimal designs are both five-level designs). Points compared for *MSE* and *RE* were the design points. It can be seen that all models perform well in all categories, with high R^2 values and low *MSE* and *RE*. The central composite design (CCD) was chosen, because this design is perhaps the most commonly used due to its ability to fit a second order response surface well [3].

While single number error metrics are easy to calculate and compare, another concern in the computation of error in multi-dimensional design is the determination of model accuracy relative to the location in the model space. In this case error might be imagined as a vector that is

Table A1 Summary of error metrics for two-input-parameter designs.

Design	CCD	D-Optimal	Taguchi	3-Level Factorial
R^2	1.00	1.00	0.98	1.00
Adj R^2	1.00	1.00	0.96	0.99
MSE	0.69 %	0.13 %	0.48 %	0.10 %
RE	1.10%	0.17 %	0.64 %	0.14 %

"tacked" at some point, with magnitude and direction. One method of characterizing and locating error is the reservation of a few runs expressly for the purpose of characterizing model error. Often RSM designs reserve runs in the form of replicates of design points, which is useful in a stochastic setting, such as conducting physical experiments, but not in a deterministic simulation environment.

Stiffness and location errors were calculated for all points in the face centered cubic design space discussed in Chapter 3 (25). Then error surfaces were fit for both of these error features. The error should be nonsystematic and small, however for response surface models it is expected that error will be smaller near the design points and larger "far away." A high R^2 on location error indicated a good fit and that error for this variable was likely to be systematic in some way. On the other hand, a relatively low R^2 on stiffness error indicated that it was not possible to adequately fit a cubic surface to the data, indicating that either the stiffness error is highly nonlinear in nature or very non-systematic. Either another fitting scheme must be used with more "error points" reserved, or some other method must be used to estimate the error on stiffness predictions.

Shown below is the location error surface developed. An error criterion could be chosen and only those points passing the error criterion would be saved. In a sense, the model would be valid for these locations only. Elsewhere, the model would not do a good enough job of estimating according to the interpolated surface. This would indicate to the analyst those regions of the model with adequate goodness of fit and those regions of the model with poor goodness of fit. Again, this work is not concerned with actually assigning an error criterion and determining where the model is valid, as this would be application dependent and the 5DOF system is only a simple theoretical problem.

DESIGN-EXPERT Plot
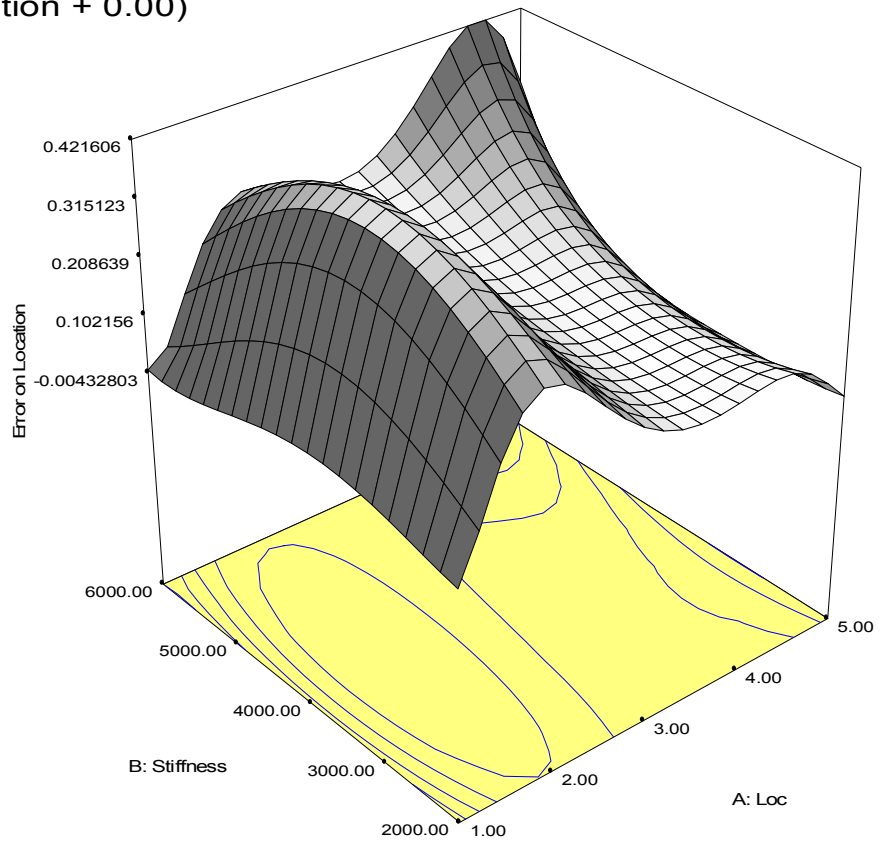
Sqrt(Error on Location + 0.00)
X = A: Loc
Y = B: Stiffness

Figure A1: Location Error Surface

Appendix B

ATTEMPTS TO SOLVE THE INVERSE PROBLEM USING TIME SERIES FEATURES

The time series features ET and LD were used in the first attempt at the solution of the inverse problem. Time series features were used in anticipation of eventually solving a nonlinear problem, where frequency domain features might be difficult to derive. However, as shown in Chapter 3, these features are highly correlated, and so non-unique solutions were obtained. Following is an explanation of the steps taken to arrive at this conclusion.

Optimization schemes were implemented for the solution of the inverse problem, that is the question "Knowing what the time series output features are, can the system input parameters that caused such outputs be determined?" had to be answered. Because of the nonfunctional nature of the inverse problem, optimization seemed a natural choice for its solution. Matlab™'s *fminsearch* routine, which uses Nelder Meade simplex unconstrained nonlinear optimization [20], was implemented. Four features were used as constraints, implemented in the form of an error function that was to be minimized. They were the LD and E features from Location 3 and the LD and E features from Location 5. Additional constraints were that three of the input parameters were fixed or considered "known" (mass, impulse magnitude and impulse location), reducing the size of the inverse problem to a one-dimensional optimization.

The starting value for stiffness was randomly generated between its upper and lower bounds. Then the optimization routine worked to minimize the error between the actual and predicted values of the output feature. The response surface relationships generated with the CCD given in Chapter 3 along with the fixed mass, impulse magnitude and impulse location, and the changing stiffness value were used to obtain predicted output feature values. The squared error between actual and predicted was weighted by the inverse variance between the features, which causes more weight to be placed on values with small variance. In theory, smaller variance on a feature should correspond to higher confidence that this feature is known well. More weight on this well- known feature emphasizes it in the optimization process.

Fifty local minima were found using fifty random start points per run. Global minima were defined as the local minima with the lowest objective function values. Unfortunately many points were often "tied" for this honor, implying that several values for stiffness, combined with the other three fixed input parameters, could result in a particular combination of output feature values. The conclusion was that different output features were needed and a different optimization scheme as well, one that would allow a ranking of points.

Appendix C

BEAM DESIGN POINT SIMULATION RUNS

Beam-mass design points are shown on the following pages. Input parameters were whether a mass was present at each of the ten locations, output features were the simulated frequencies, in Hz, of the first ten beam modes. The design consists of 32 runs, or $1/32^{nd}$ of the full factorial set of 1024 runs.

Input Parameters

(Mass Present at Location)　　　　**Output Features (Frequencies derived from simulation, Hz)**

Design point	L1	L2	L3	L4	L5	L6	L7	L8	L9	L10	ω_1	ω_2	ω_3	ω_4	ω_5	ω_6	ω_7	ω_8	ω_9	ω_{10}
1	0	0	0	0	0	1	1	1	1	1	3.42	17.87	56.01	117.65	179.65	269.11	398.91	508.58	634.46	839.89
2	1	0	0	0	0	0	0	0	0	1	3.26	20.72	60.94	134.62	207.47	323.97	463.54	573.03	756.05	949.79
3	0	1	0	0	0	0	0	0	1	0	3.34	21.30	67.21	128.71	199.65	314.26	411.29	601.42	749.46	982.85
4	1	1	0	0	0	1	1	1	0	0	2.72	17.28	62.34	114.69	185.28	282.19	390.81	529.73	682.07	852.50
5	0	0	1	0	0	0	0	1	0	0	3.40	21.89	67.54	115.98	209.30	303.32	469.11	577.40	733.85	915.98
6	1	0	1	0	0	1	1	0	1	0	2.79	17.69	57.26	110.27	171.25	302.93	401.59	527.27	689.19	774.76
7	0	1	1	0	0	1	1	0	0	1	2.86	18.91	57.05	113.86	180.13	273.68	403.23	494.87	656.70	822.79
8	1	1	1	0	0	0	0	1	1	1	2.64	17.05	56.86	108.98	183.26	266.85	400.80	496.35	638.58	794.86
9	0	0	0	1	0	0	1	0	0	0	3.44	22.42	64.28	115.85	214.70	319.46	423.52	580.78	747.16	982.88
10	1	0	0	1	0	1	0	1	1	0	2.86	17.51	54.84	112.21	181.85	299.02	387.35	492.48	739.40	807.58
11	0	1	0	1	0	1	0	1	0	1	2.94	18.76	55.47	112.8	182.69	257.35	341.70	505.47	771.14	910.35
12	1	1	0	1	0	0	1	0	1	1	2.66	17.12	52.93	109.53	179.72	265.03	362.46	531.98	633.93	852.20
13	0	0	1	1	0	1	0	0	1	1	3.02	19.44	54.22	114.13	170.96	290.22	375.44	527.51	674.48	778.53
14	1	0	1	1	0	0	1	1	0	1	2.69	17.36	53.14	100.28	188.11	269.02	390.92	518.19	621.22	800.36
15	0	1	1	1	0	0	1	1	1	0	2.55	17.27	60.33	105.52	177.18	281.67	384.09	506.76	638.52	807.19
16	1	1	1	1	0	1	0	0	0	0	2.50	20.25	58.34	111.95	188.19	288.47	375.70	552.12	654.43	845.79
17	0	0	0	0	1	1	0	0	0	0	3.47	22.70	62.04	132.16	204.70	310.30	426.65	590.94	730.94	902.69
18	1	0	0	0	1	0	1	1	1	0	2.93	16.94	56.94	113.22	193.05	278.39	386.39	554.23	650.63	817.03
19	0	1	0	0	1	0	1	1	0	1	3.02	18.13	56.43	113.14	188.66	242.16	394.93	524.54	621.49	922.74
20	1	1	0	0	1	1	0	0	1	1	2.67	17.14	50.43	122.24	172.82	269.69	372.70	531.78	640.63	803.86
21	0	0	1	0	1	0	1	0	1	1	3.11	18.82	54.79	112.64	174.67	256.62	381.55	567.31	614.96	898.82
22	1	0	1	0	1	1	0	1	0	1	2.70	17.42	51.27	109.11	172.50	251.00	409.40	513.31	602.08	869.40
23	0	1	1	0	1	1	0	1	1	0	2.75	18.16	56.46	113.22	165.29	270.66	373.21	481.25	593.63	777.92
24	1	1	1	0	1	0	1	0	0	0	2.55	19.27	59.51	110.33	187.56	265.44	421.07	493.88	691.69	900.82
25	0	0	0	1	1	0	0	1	1	1	3.20	18.83	53.57	112.14	192.98	265.50	402.89	499.52	640.55	828.85
26	1	0	0	1	1	1	1	0	0	1	2.73	17.59	50.36	109.62	185.21	272.50	400.11	493.99	639.20	808.01
27	0	1	0	1	1	1	1	0	1	0	2.77	18.52	55.18	112.25	173.77	257.65	361.99	459.19	680.40	794.71
28	1	1	0	1	1	0	0	1	0	0	2.61	18.94	56.29	113.13	193.84	274.69	386.63	527.97	692.27	871.61
29	0	0	1	1	1	1	1	1	0	0	2.80	19.34	58.37	104.62	176.49	267.29	369.89	510.80	625.82	778.13
30	1	0	1	1	1	0	0	0	1	0	2.67	19.40	52.67	117.29	180.49	296.17	401.39	527.75	685.27	779.62
31	0	1	1	1	1	0	0	0	0	1	2.73	20.92	54.10	122.00	183.26	263.61	398.36	500.56	653.18	837.66
32	1	1	1	1	1	1	1	1	1	1	2.33	15.26	47.08	97.743	159.03	230.73	328.45	443.40	552.97	679.97

Vita

Mandy Cundy was born on February 3, 1979 to Vic and Karin Cundy of Bozeman, Montana. She graduated from Bozeman High School in 1997 and started at Montana State University as a Presidential Scholar in the Civil Engineering Department that year. She earned her Bachelor of Science in Civil Engineering and an Honors Degree in May 2001. Mandy began her thesis research in January 2002 with Dr. Dan Inman at Virginia Tech in the area of response surface analysis and its applications to structural dynamics problems. She has been employed summers and internship semesters for the last five years at Los Alamos National Laboratory, where she is returning to work in January 2003 as a Technical Staff Member.

Address: Los Alamos National Laboratory
Engineering Sciences and Applications Division, Weapons Response, M/S P946
PO Box 1663
Los Alamos, New Mexico 87545
cundy@lanl.gov